the presence of BALF. Negative values for GM-CSF bioactivity in BALF are hereafter referred to as the neutralizing capacity of BALF.

Quantification and purification of anti–GM-CSF autoantibodies

Anti–GM-CSF autoantibodies (autoantibodies) were purified from the sera of iPAP patients as previously described.[32,33] Antibody concentrations were measured in BALF or serum using purified autoantibodies as a standard, according to the method reported previously.[32,33]

Confocal microscopy

Lung tissues resected from an iPAP patient or a healthy control were fixed in periodate-lysine-paraformaldehyde (PLP).[34] Sections were incubated in phosphate-buffered saline (PBS) containing 1% bovine serum albumin (BSA), immunostained with fluorescein isothiocyanate (FITC)–labeled antihuman immunoglobulin G (IgG; BD Biosciences, San Jose, CA) or with phycoerythrin (PE)–labeled GM-CSF (R&D Systems), and examined by confocal laser microscopy (Carl Zeiss, Tokyo, Japan). Serial sections from an iPAP patient was immunostained with FITC-labeled antimurine IgG (Nichirei) and PE-labeled G-CSF (R&D Systems) to exclude nonspecific binding. Hematoxylin-eosin was used for counterstaining.

GM-CSF autoantibody immune complexes

BALF from iPAP patients or healthy controls was delipidated with 1-butanol, and the protein fraction was precipitated with cold acetone. The protein pellet was resuspended in PBS, incubated with protein-A Sepharose 4 Fast Flow (Amersham Biosciences, Buckinghamshire, United Kingdom; 4°C, overnight), and washed with PBS/0.1% Tween 20. Bound proteins were eluted with glycine-HCl (100 mM, pH 2.7) and reprecipitated with 80% cold acetone. Bound and unbound protein fractions were size fractionated by sodium dodecyl sulfate–polyacrylamide gel electrophoresis (SDS-PAGE) under reducing conditions and were transferred to polyvinylidene fluoride membranes (Millipore, Bedford, MA), and GM-CSF was detected using rabbit antihuman GM-CSF antibodies (1:1000; R&D Systems), horseradish peroxidase-conjugated goat antirabbit IgG antibodies (1:100; Nichirei), and ECL Plus (Amersham Pharmacia Biotech, Buckinghamshire, United Kingdom).

Delipidated BALF proteins were subjected to PAGE under nonreducing conditions, followed by Western blot analysis as described. IgG in the BALF proteins was also detected by Western blot analysis using horseradish peroxidase-conjugated goat antihuman IgG (1:3000; DAKO) and ECL Plus.

BALF (100 μL) from iPAP patients or healthy controls was incubated with [^{125}I]–GM-CSF (0.03 pmol; 2 hours, room temperature) and then subjected to PAGE under nonreducing conditions followed by autoradiography.

Characterization of autoantibodies

GM-CSF binding avidity and capacity of purified autoantibodies were determined using the [^{125}I]–GM-CSF binding assay method of Svenson et al.[35] Briefly, sera IgG from iPAP patients were isolated by protein-G Sepharose column chromatography (Amersham Biosciences) and quantified as described. Autoantibodies from each person were analyzed separately. Calculations were performed using molecular weights of 14.7 and 146 kDa for rhGM-CSF and IgG, respectively, and the results were expressed in picomolars. The binding capacity (B_{max}, sites/mol IgG) was determined from the plateau value of the saturation-binding plot. The average affinity (K_{AV}) was defined as the concentration of free GM-CSF at 50% B_{max}.

The binding specificity of autoantibodies for GM-CSF was determined using sandwich enzyme-linked immunosorbent assay (ELISA). Micro-ELISA plates (Nunc, Roskilde, Denmark) were coated with rhGM-CSF produced in *E coli* (as a standard) or GM-CSF produced in CHO cells, the large trypsin fragment of rhGM-CSF, carboxymethylated rhGM-CSF, murine or bovine GM-CSF, or various human cytokines (all at 1 μg/mL) overnight, and then with 1% BSA/PBS. Plates were then incubated with purified autoantibody (100 ng/mL) for 1 hour. The reactivity of the autoantibodies in each well was measured by the method described above and was expressed as an OD ratio to that of *E coli*-derived rhGM-CSF.

The GM-CSF-neutralizing capacity of autoantibodies was determined as previously described using a bioassay based on GM-CSF–stimulated proliferation of TF-1 cells.[22,30] Briefly, TF-1 cells (4×10^4 cells/well) were cultured (37°C, humidified atmosphere, 5% CO_2) for 3 days in medium containing rhGM-CSF (5 ng/mL) and various concentrations of purified autoantibodies, murine antihuman GM-CSF monoclonal antibody (R&D Systems), goat antihuman GM-CSF polyclonal antibody (R&D Systems), or human IgG (Sigma-Aldrich). The percentage of growth inhibition was calculated from the following equation: Growth inhibition (%) = $100 \times (A - B)/(A - C)$, where A, B, and C are the absorbances of TF-1 cells grown with rhGM-CSF (5 ng/mL) alone, rhGM-CSF and anti–GM-CSF antibodies or the negative control, and medium alone, respectively. The concentration of each autoantibody at 50% growth inhibition (IC_{50}) was obtained from each growth inhibition curve. GM-CSF epitope mapping of autoantibodies was performed using a competitive binding assay using murine monoclonal antibodies that recognize specific regions of human GM-CSF.[28] Purified autoantibodies (0-1 μg/mL) were mixed individually with the murine monoclonal anti–GM-CSF epitope-specific antibodies 4117, 1089, 3092, and 1022 (each at 1 μg/mL). These murine antibodies recognize rhGM-CSF residues 1-11, 40-77, 78-94, and 110-127, respectively.[28] Polyclonal rabbit anti–GM-CSF peptide 54-73 was used as a positive control, and human IgG (Sigma-Aldrich) was used as a negative control. Antibody mixtures were then incubated (4°C, overnight) in PBS containing [^{125}I]–GM-CSF (1 ng/mL), 2% BSA, and 0.1% Triton X-100. Mixtures were then transferred to individual wells of a 96-well plate (FlashPlate Plus; Perkin-Elmer, Boston, MA) that had been previously coated with goat antimouse IgG and plastic scintillant. Plates were incubated (room temperature, 2 hours) and washed in PBS/0.1% Tween 20, and bound radioactivity was counted in a TopCount NXT Microplate Scintillation and Luminescence Counter (Perkin-Elmer). The ability of autoantibodies to inhibit the binding of GM-CSF region-specific monoclonal antibodies was determined using the following formula: Binding inhibition (%) = $100 \times [Cpm(A) - Cpm(B)]/[Cpm(A) - Cpm(C)]$, where Cpm(A) is the radioactivity in wells containing murine monoclonal antibody and [^{125}I]–GM-CSF but no autoantibodies; Cpm(B) is the radioactivity in wells containing autoantibodies, murine monoclonal antibody, and [^{125}I]–GM-CSF; and Cpm(C) is the radioactivity in wells containing [^{125}I]–GM-CSF but neither murine monoclonal antibody nor autoantibodies.

Statistical analysis

Statistical analyses were performed on a microcomputer using StatView (version 4.0) (Abacus Concepts, Berkeley, CA) using the Mann-Whitney U test or the Kruskal-Wallis rank sum procedures for nonparametric data. $P < .05$ was considered significant.

Results

AM growth and development are inhibited by iPAP bALF

As shown in Table 1, BALF from patients with iPAP contained fewer AMs and increased the number of lymphocytes compared with that from age-matched healthy subjects. AMs isolated from iPAP BALF by plastic adhesion had "monocyte-like" morphology and were smaller than those from healthy controls (Figure 1A). To determine whether an inhibitory activity for AM growth or function is present in the iPAP lung, we incubated AMs from iPAP patients in the presence of culture medium alone or medium plus iPAP- or control-BALF in the absence or presence of GM-CSF (20 ng/mL). AMs from iPAP patients were viable but remained small after 14 days in culture with medium alone or in medium containing iPAP-BALF (Figure 1B). In contrast, iPAP-AMs developed a normal appearance and were larger in medium containing normal

Table 1. Cellular constituents in the BALF

	No. subjects	Sex, F/M	Median age, y	Median BAL recovery, %	Median BAL cell density, $\times 10^4$/mL	Median cell differentials							
						Macrophage		Lymphocyte		Neutrophil		Eosinophil	
						No., $\times 10^4$/mL	%	No., $\times 10^4$/mL	%	No., $\times 10^4$/mL	%	No., $\times 10^4$/mL	%
Patients with iPAP	34	10/24	52 (28-79)	70.2 (48.7-73.3)	10.5 (2.8-55.9)	4.2 (2.17-26.5)*	60.0 (5.9-90.9)*	3.2 (0.5-52.6)*	32.5 (6.8-94.1)*	0.3 (0.0-4.8)	2.3 (0.0-15.0)*	0.0 (0.0-0.3)	0.3 (0.0-6.3)
Control	18	10/8	50 (27-72)	67.0 (59.3-77.0)	14.0 (3.8-42.2)	13.2 (3.3-39.8)	93.3 (84.0-96.8)	0.8 (0.2-3.1)	6.0 (2.9-14.0)	0.1 (0.0-0.4)	0.3 (0.0-2.0)	0.0 (0.0-0.2)	0.0 (0.0-1.0)

Numbers in parentheses are ranges.
*$P < .05$ compared with control.

BALF with or without added GM-CSF. Although iPAP-AMs failed to grow and develop a normal appearance in medium plus iPAP-BALF, they did so when additional GM-CSF (20 ng/mL) was added. The effects of control-BALF or GM-CSF on iPAP-AM growth were confirmed with an MTT assay (data not shown). Cell viability in each instance was greater than 90%. These data establish that GM-CSF bioactivity is reduced in the iPAP-BALF by an inhibitory substance that can be overcome with the addition of GM-CSF.

Pulmonary GM-CSF expression is not diminished in iPAP

Functional GM-CSF activity appeared to be absent in BALF from iPAP patients, but it could be restored with the addition of large amounts of GM-CSF to medium containing iPAP BALF. Therefore, we evaluated GM-CSF levels in lung tissues from 4 iPAP

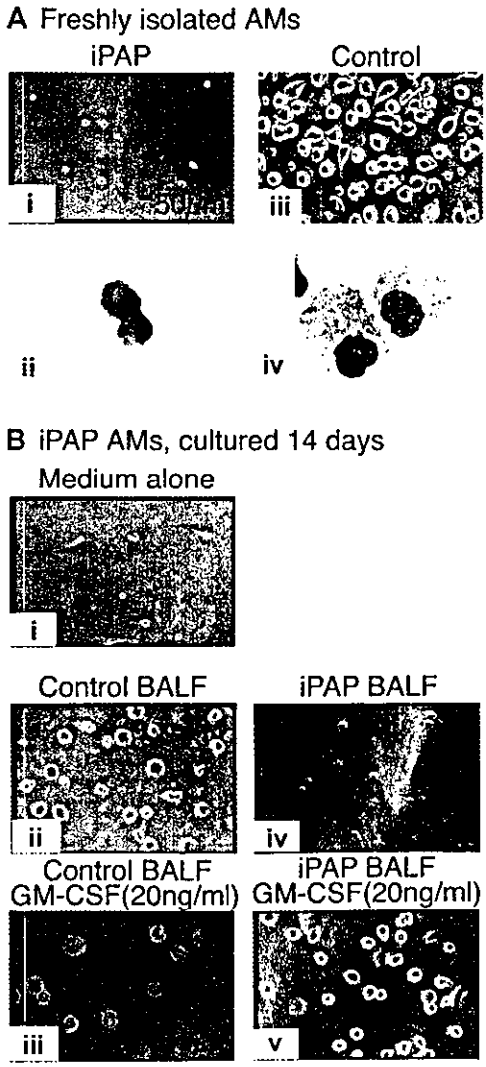

Figure 1. Morphology and in vitro growth of adherent AMs from a patient with iPAP. (A) Adherent AMs from a patient with iPAP and a healthy subject. iPAP AMs showed a small, monocyte-like appearance with basophilic cytoplasm (phase-contrast micrograph [i], original magnification × 200; and Wright-Giemsa staining [ii], original magnification × 1000), whereas those from control-BALF had large eosinophilic cytoplasm (phase-contrast micrograph [iii], original magnification × 200; and Wright-Giemsa staining [iv], original magnification × 1000). (B) After incubation with control-BALF for 14 days, iPAP-AM size increased markedly (ii) (original magnification × 200) compared with before incubation (Ai) or incubation with medium alone (i), and adding 20 ng/mL GM-CSF further promoted growth (iii). After incubation with iPAP-BALF, AMs remained small (iv), but adding 20 ng/mL GM-CSF restored their growth (v).

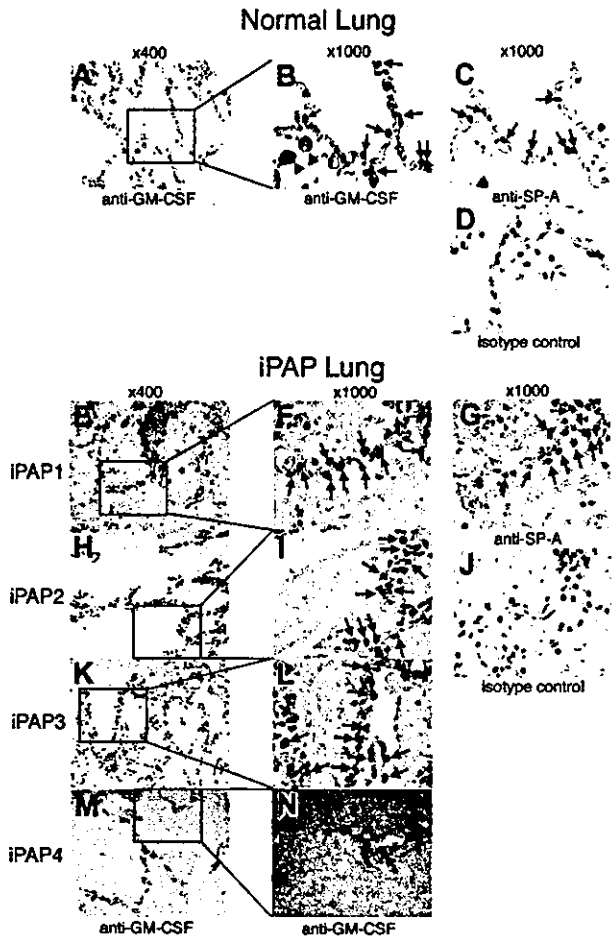

Figure 2. Immunohistochemical detection of GM-CSF in the lungs of patients with iPAP. Lung tissue biopsy specimens from 4 patients with iPAP or 4 healthy controls were assessed for the presence of GM-CSF and SP-A by immunohistochemical staining. (A-D) Sections of normal lung. AM (B, arrowheads) and alveolar epithelial cells (B, arrows) were stained red by anti–GM-CSF antibody (A-B). Alveolar epithelial cells stained by anti–GM-CSF antibodies were stained brown by anti–SP-A antibodies on the serial section (C, arrows). Therefore, they were likely to be alveolar type 2 cells. (E-N) Sections of iPAP lung. Alveolar epithelial cells (F, I, L, N, arrows) stained red. Similar cells were stained brown on the serial section (G, arrows). Original magnifications are indicated above each column.

patients and 4 controls using an immunohistochemical approach. Epithelial cells projecting into the alveolar lumen were strongly stained with anti–GM-CSF antibody in iPAP and control lungs (Figure 2). These cells were also stained with anti–SP-A antibody, establishing that they are alveolar type 2 epithelial cells. The proportion of alveolar epithelial cells showing GM-CSF expression was evaluated by immunohistochemistry, with similar percentages found for iPAP patients (n = 4; 50.5% ± 8.4%) and controls (n = 4; 40.8% ± 5.0%) (P = .08). Thus, GM-CSF protein production in the lungs of iPAP patients does not appear to be reduced compared with normal lungs.

GM-CSF bioactivity is reduced in the lungs of iPAP

Discordance between the physical presence and functional activity of GM-CSF was apparent in the BALF of iPAP patients but not in controls. Therefore, we measured the bioactivity of GM-CSF in BALF using a bioassay based on GM-CSF–dependent growth stimulation of TF-1 cells.[22,30] Increasing concentrations of GM-CSF stimulated an increasing proliferation of TF-1 cells, reaching a maximum at very low doses on the order of 2 to 3 ng/mL (Figure 3A). Adding BALF from healthy controls (n = 6; 20% vol/vol) had no effect on the survival of TF-1 cells at equivalent doses of exogenous GM-CSF, suggesting that neither large amounts of GM-CSF nor GM-CSF inhibitory activity was present (Figure 3B). In contrast, adding BALF from iPAP patients (n = 8; 20% vol/vol) shifted the viability curve significantly to the right, demonstrating the presence of a potent GM-CSF–inhibitory activity (Figure 3B). Importantly, the GM-CSF–inhibitory activity was reversible as maximum survival was achieved with high doses of exogenous GM-CSF (20 ng/mL). GM-CSF bioactivity in BALF was −24.9 ± 16.4 ng/mL (median, −23.3; range, −57.5 to −4.3) for iPAP and 0.017 ± 0.387 ng/mL (median, −0.126; range, −0.34 to 0.63) for healthy controls (Figure 3C). We also determined GM-CSF levels in control BALF to be 1.07 ± 0.16 pg/mL (range, 0.88-1.28) using an ELISA system (AN'ALYSA; R&D Systems), so GM-CSF–neutralizing capacity in iPAP-BALF was present in vast excess over the levels of GM-CSF normally present within the lung.

Autoantibodies occur at high levels in patients with iPAP

We sought to extend and quantify our observation regarding the presence of autoantibodies (anti–GM-CSF autoantibodies) in iPAP

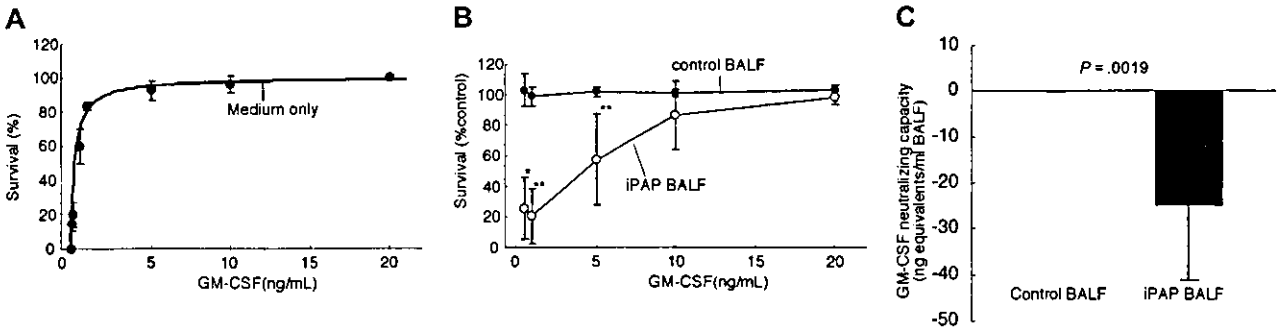

Figure 3. GM-CSF bioactivity is severely reduced in the lungs of iPAP patients. (A) Bioassay used to quantify GM-CSF bioactivity in BALF. TF-1 cells survived and proliferated in a dose-dependent fashion in the presence of GM-CSF added to the culture medium. Each point represents the mean of 6 determinations. (B) Quantification of inhibition of GM-CSF bioactivity by BALF of iPAP patients. Addition of 20% (vol/vol) BALF from healthy control subjects (closed symbols, n = 6 per point) or iPAP patients (open circles, n = 8 per point). Compared with cells cultured with medium without BALF (as in panel A), adding BALF from healthy controls had no measurable effect on the GM-CSF–dependent survival of TF-1 cells. In contrast, iPAP-BALF significantly inhibited GM-CSF–dependent survival of TF-1 cells (**P < .002 or *P < .05). This inhibitory effect was overcome by the addition of large amounts of GM-CSF to the medium. (C) Deficit of pulmonary GM-CSF bioactivity in iPAP. The bioactivity of GM-CSF in BALF from healthy controls or iPAP patients was calculated as described in "Patients, materials, and methods" and was shown as aggregate data in panel B. The deficit in GM-CSF bioactivity is expressed in nanogram of GM-CSF per milliliter of BALF. Error bars indicate SD.

Table 2. High levels of anti–GM-CSF autoantibodies in iPAP patients

Sample	iPAP median, μg/mL	Healthy control* median, μg/mL	Other lung disorders* median, μg/mL
BALF	1.15 (0.094-5.40), n = 34	< 0.050, n = 18	< 0.050, n = 14
Serum	88.6 (16.6-470), n = 107	< 3.00, n = 19	< 3.00, n = 10

Numbers in parentheses are ranges.
*Concentrations of autoantibodies in BALF and serum were all under the detection limit (0.05 μg/mL in BALF; 3 μg/mL in serum).

in a large cohort. Therefore, the levels of autoantibodies were quantified by ELISA in the BALF and sera of patients with iPAP or other lung disorders and in healthy controls. BALF and sera of iPAP patients contained high concentrations of autoantibodies (median, 1.15; range, 0.09-5.40 μg/mL in BALF [n = 34]; median, 88.6; range, 16.6-470 μg/mL in sera [n = 107], respectively) in contrast to healthy controls and patients with other lung diseases that were all under the detection limit (0.05 μg/mL for BALF and 3 μg/mL for serum) (Table 2). Thus, autoantibody levels are high in the lungs and sera of patients with iPAP and are specific for this disorder.

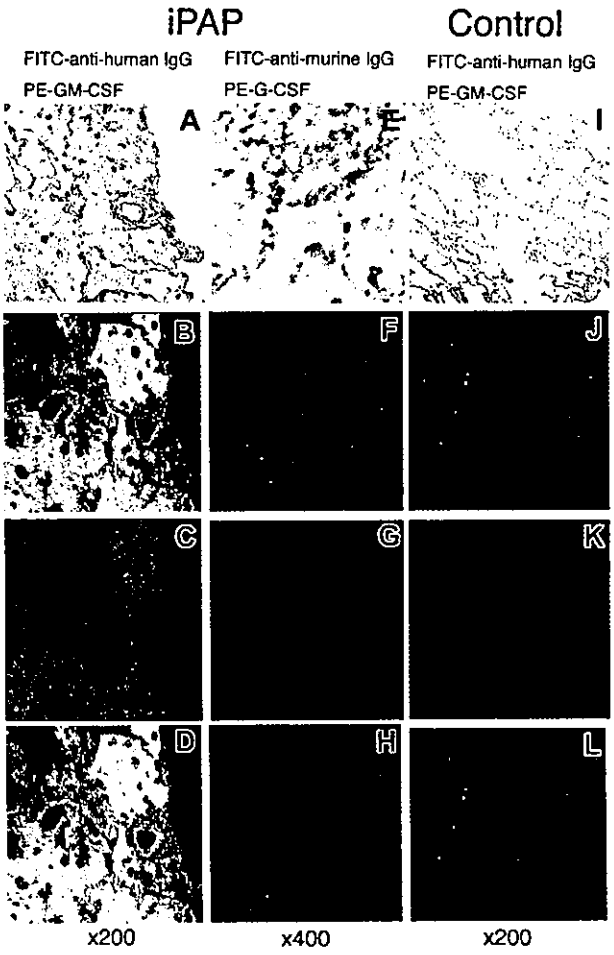

Figure 4. Confocal microscopic images of immunohistochemical double staining for the autoantibodies against GM-CSF. (A-H) Lung tissue from a patient with iPAP. (I-L) Histologically normal lung tissue from a patient with lung cancer. These tissues were stained with hematoxylin-eosin (A, E, I), FITC-conjugated antihuman IgG (green; B, J), FITC-conjugated antimurine IgG (green; F), PE-conjugated GM-CSF (red; C, K), and PE-conjugated G-CSF (red; G). A combination of both channels (B-C, F-G, J-K) clearly demonstrates the occurrence of the autoantibodies in the alveolar filling materials of the iPAP lung (D) but not in normal lung (L).

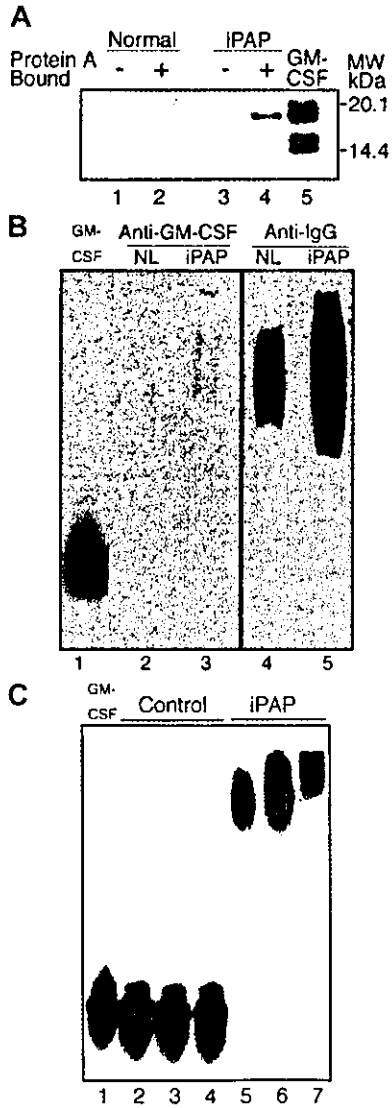

Figure 5. Formation of GM-CSF–autoantibody immune complexes in iPAP patients. (A) Detection of GM-CSF containing immune complexes in the BALF in iPAP by immunoprecipitation. Protein A Sepharose beads were incubated with BALF from a healthy control (lanes 1-2), iPAP patient (lanes 3-4), or, as a control, purified yeast-derived rhGM-CSF (lane 5). Bound and unbound fractions (indicated) were separated and subjected to SDS-PAGE under reducing conditions and Western blotting using a rabbit anti–GM-CSF antibody. Under these conditions, the rhGM-CSF standard consists of 3 molecular species migrating at 19.5, 16.8, and 15.5 kDa. (B) Detection of GM-CSF and IgG in BALF by Western blotting. BALF from a healthy control (lanes 2, 4), iPAP patient (lanes 3, 5), or rhGM-CSF (lane 1) was subjected to native PAGE and then Western blotting using a rabbit anti–GM-CSF antibody (lanes 1-3) or anti-IgG antibody (lanes 4-5). (C) Supershift of [^{125}I]–GM-CSF with iPAP-BALF. BALF from healthy controls (lanes 2-4) or iPAP patients (lanes 5-7) was incubated with [^{125}I]–GM-CSF and then subjected to native PAGE and autoradiography. As a control, [^{125}I]–GM-CSF alone was also included on the gel (lane 1).

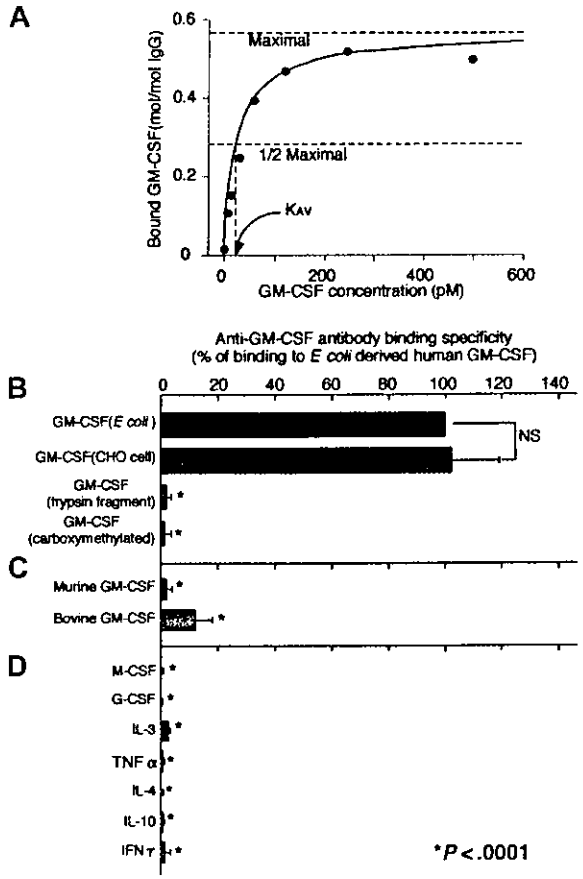

Figure 6. Binding affinity, capacity, and specificity of purified anti–GM-CSF autoantibodies in iPAP patients. (A) Saturation binding plot of [^{125}I]–GM-CSF binding to purified anti–GM-CSF autoantibody. Vertical axis represents the molar fractional binding of GM-CSF to autoantibody. Binding capacity (maximal binding) was determined from the asymptote of the curve, and binding affinity (K_{AV}) was determined from the concentration of GM-CSF at 50% of maximum binding. (B) Binding of autoantibodies to various forms of human GM-CSF. Reactivity of autoantibodies was measured by antigen capture and compared with binding to recombinant human GM-CSF produced in *E coli*, which was taken as 100%. Various forms were tested, including recombinant human GM-CSF produced in CHO cells; the large trypsin fragment that contained residues 31-58, 86-107, and 112-127, connected by disulfide bonds; and carboxymethylated GM-CSF, which had an intact primary amino acid sequence but lost the second and tertiary structure because of the loss of the 2 disulfide bonds. NS indicates not significant. (C) Xenospecificity of autoantibody binding. Reactivity of autoantibodies to murine and bovine GM-CSF was measured as above. (D) Specificity of autoantibody binding with respect to other human cytokines. Reactivity of autoantibodies to various human cytokines was measured as above. Error bars indicate SD.

Localization of free autoantibodies in the lung of iPAP patients

To demonstrate that GM-CSF–binding activity colocalized with immunoglobulin molecules in the lungs of iPAP patients, immunohistochemical staining was carried out with PE-conjugated GM-CSF and FITC-conjugated anti-IgG. By confocal microscopy, GM-CSF–binding activity and IgG were readily detected and demonstrated strong colocalization in the iPAP lung (Figure 4A-D). Nonspecific binding of PE- or FITC-conjugated proteins on the intra-alveolar material was ruled out by staining of the serial sections with FITC-conjugated antimurine-IgG and PE-conjugated human G-CSF (Figure 4E-H). The lungs of healthy controls had detectable, but vastly reduced, amounts of IgG, minimal or no GM-CSF–binding activity, and no colocalization (Figure 4I-L).

Autoantibodies form immune complexes in the lungs of iPAP patients

We next sought evidence of immune complexes containing GM-CSF by immunoprecipitation from BALF using protein-A Sepharose beads followed by Western blotting to detect GM-CSF. GM-CSF was detected in iPAP-BALF in the protein-A bound, but not unbound, fraction, consistent with the presence of GM-CSF bound to IgG (Figure 5A). GM-CSF was not detected in either fraction in BALF from healthy controls. When the BALF protein was evaluated by native gel electrophoresis and Western blotting, GM-CSF was also detected as a broad high-molecular-weight smear that coincided with a similar smear detected by blotting for IgG (Figure 5B). Using yet another approach, a "supershift" of GM-CSF was seen after incubation of [^{125}I]–GM-CSF with iPAP-BALF but not with control-BALF (Figure 5C). Using several distinct experimental approaches, these data strongly support the notion that GM-CSF exists in the form of immune complexes in the lungs of iPAP patients.

Autoantibodies bind GM-CSF with high avidity and specificity

The absence of detectable GM-CSF bioactivity in BALF from iPAP patients suggested that the binding affinity of autoantibodies for GM-CSF might be sufficient to effectively compete for the binding of GM-CSF to its receptor. Thus, autoantibody binding avidity and capacity was determined by saturation-binding analysis using purified autoantibodies and [^{125}I]–GM-CSF (Figure 6A). Autoantibodies purified from 11 iPAP patients had a similar, high avidity (19.96 ± 7.54 pM) in contrast to that of a commercial goat polyclonal antibody (275.4 pM) (Table 3). The binding capacity of autoantibodies from a range of iPAP patients was similar, with 0.24 ± 0.13 sites/mol IgG, indicating that 1.8 to 7.8 autoantibody molecules bound each molecule of GM-CSF (Table 3). Consistent with these avidity data, the autoantibodies exhibited strong neutralizing capacity. The mean neutralizing capacity of autoantibodies was 10- to 500-fold greater than those of the commercial neutralizing polyclonal or monoclonal antibodies tested, respectively (Table 3).

Table 3. K_{AV}, B_{max}, and IC_{50} of autoantibodies from patients with iPAP

Patient	K_{AV} avidity, pM	B_{max} capacity, sites/mol IgG	IC_{50}, mol/mol rhGM-CSF
1	20.1	0.129	5.84
2	13.3	0.153	4.43
3	16.7	0.168	3.83
4	24.9	0.253	6.65
5	11.1	0.134	8.66
6	24.8	0.332	6.65
7	12.1	0.194	2.42
8	15	0.184	11.88
9	22.3	0.565	2.42
10	37	0.273	12.08
11	22.3	0.281	12.69
Average ± SD	19.96 ± 7.54	0.24 ± 0.13	7.05 ± 3.81
Commercialized goat anti–GM-CSF*	275.4	0.402	74.91
Commercialized murine anti–GM-CSF*	ND	ND	> 4000

ND indicates not determined.
*Neutralizing antibodies.

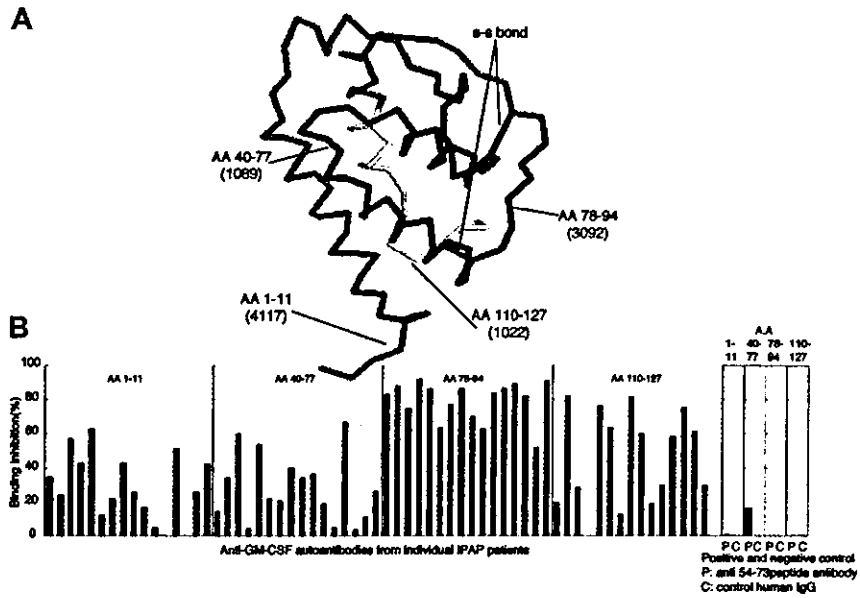

Figure 7. Epitope targeting of the autoantibodies on the GM-CSF molecule. (A) Three-dimensional diagram of GM-CSF showing the 4 regions covered by the murine monoclonal antibodies used for epitope mapping of autoantibodies isolated from iPAP patients. Murine antibodies and the epitopes on human GM-CSF they recognize included 4117 (residues 1-11), 1089 (residues 40-77), 3092 (residues 78-94), and 1022 (residues 110-127), respectively. (B) Competitive GM-CSF binding assay of the autoantibodies with epitope-specific murine monoclonal antibodies. Each bar indicates the percentage of inhibition of [^{125}I]–GM-CSF binding to each monoclonal antibody by the autoantibodies from each patient with iPAP. Percentage of inhibition for the reactions without the autoantibodies and without monoclonal antibody was defined as 0% and 100% inhibition, respectively. Control human IgG and rabbit anti–GM-CSF peptide 54-73 polyclonal antibodies were used for negative and positive controls, respectively. Distribution of the percentage of inhibition was variable among the patients, but the autoantibodies consistently and strongly inhibited GM-CSF binding to the monoclonal antibody 3092.

The binding of autoantibodies to GM-CSF was also specific. Purified autoantibodies from 12 iPAP patients showed similar binding to rhGM-CSF prepared in *E coli* (nonglycosylated) and CHO cells (glycosylated), indicating the carbohydrate moiety was not involved in binding (Figure 6B). Autoantibodies did not bind GM-CSF that had been carboxymethylated (which disrupts disulfide bonds), suggesting that a secondary or tertiary structure may be recognized. Autoantibodies did not bind GM-CSF after trypsin cleavage, which retains the 2 disulfide bonds but not peptides 1 to 30, 59 to 85, and 108 to 111, suggesting that these peptides may contain critical binding epitopes (Figure 6B). Autoantibodies bound bovine GM-CSF, which has 68% amino acid homology with human GM-CSF, but not murine GM-CSF, which has only 53% homology (Figure 6C). None of a large variety of cytokines tested was bound by autoantibodies (Figure 6D). These findings demonstrate that autoantibodies consistently bind GM-CSF with high avidity and specificity and likely recognize a secondary or tertiary, nonglycosylated portion of the molecule.

Autoantibodies target a functional domain of GM-CSF

The specific epitopes on GM-CSF recognized by autoantibodies were identified using a competitive binding assay with [^{125}I]–GM-CSF and 4 different epitope-specific murine monoclonal antibodies (Figure 7A). Monoclonal antibodies recognizing GM-CSF amino acids 1 to 11, 40 to 77, and 110 to 127 exhibited variable fractional inhibition by autoantibodies from separate patients (Figure 7B). In contrast, the monoclonal antibody recognizing GM-CSF residues 78 to 94 was consistently and strongly inhibited by autoantibodies from all patients, with a mean percentage inhibition of 78.97% ± 11.71% (Figure 7B). This epitope has been reported to be an important functional domain of GM-CSF.[27,28,36,37] Thus, though autoantibodies can recognize various regions of the GM-CSF molecule, the consistent, strong targeting of an epitope known to be important for GM-CSF function strongly supports the notion that autoantibodies specifically neutralize GM-CSF in patients with iPAP.

Discussion

The present study was designed to determine the functional significance of autoantibodies in patients with iPAP and to characterize their specific molecular interactions with GM-CSF. Results demonstrate that BALF from iPAP patients strongly inhibited AM growth and development in contrast to BALF from healthy controls. This effect was caused by IgG in iPAP patients that bound GM-CSF with high avidity. GM-CSF was readily detected by immunohistochemistry in the lungs of iPAP patients. However, neutralizing capacity by the autoantibodies was in nanogram per milliliter order, which far exceeds the concentration of GM-CSF in BALF from healthy lung (ie, picogram per milliliter order). This "deficit" of GM-CSF could be overcome by the addition of excess GM-CSF, demonstrating that the neutralizing capacity was saturable. Autoantibodies colocalized with GM-CSF–binding activity in the lungs of iPAP patients. GM-CSF–autoantibody complexes were also demonstrated in BALF from iPAP patients by immunoprecipitation and Western blotting. Finally, epitope mapping demonstrated that most patients with iPAP had autoantibodies with epitopes targeting a region of GM-CSF within amino acids 78 to 94, an important functional domain. Together these data demonstrate that the neutralizing anti–GM-CSF autoantibodies in iPAP patients are functionally significant and severely impair pulmonary GM-CSF bioactivity, likely impairing the development of AM terminal maturation.

Characterization of neutralizing anti–GM-CSF autoantibodies in iPAP

Autoantibody levels were surprisingly high in most iPAP patients. Although the reasons for this are unclear, the use of a highly purified autoantibody as a standard for ELISA ensured the accuracy of these findings. One possible explanation is that an "immunologic stimulus" is continuously present in the lung or elsewhere. Improving pulmonary functions after therapeutic whole lung lavage may support this idea because it may remove such stimulus.[2] Autoantibodies bound GM-CSF with high avidity, which was far higher than that of commercially

produced anti–GM-CSF antibodies. Interestingly, the binding avidity was similar to that of anti–GM-CSF antibodies in commercial preparations of pooled IgG concentrates from healthy donors (approximately 4-11 pM).[38] The significance of the latter is unclear, but their presence is intriguing. Autoantibody avidity was also similar to that of autoantibodies directed at other cytokines including IL-1α (5.5-11 pM),[39] IL-5 (15 pM),[38] IL-10 (80-351 pM),[38] and IFN-α (30 pM).[40] The similarity of ligand binding affinity for these autoantibodies and the natural cytokine receptors[35,38-41] suggests that the autoantibodies probably are functionally important in vivo, where they would be expected to effectively compete for ligand binding, thus reducing cytokine receptor occupancy and cytokine signaling. In the case of GM-CSF, this may have pathologic significance with respect to AM function. For example, GM-CSF initially binds with low affinity (5-10 nM) to the GM-CSF receptor α chain.[42] Subsequently, this complex associates with the GM-CSF receptor β chain, which does not actually bind GM-CSF but converts the binding of the α chain to a high affinity bond (25-100 pM). The affinity of the autoantibodies (approximately 20 pM) for GM-CSF is stronger than that of the α chain. Thus, it is likely that the autoantibodies may inhibit GM-CSF signaling by blocking the initial binding to the low-affinity receptor. The presence of immune complexes consisting of autoantibodies and GM-CSF provides further strong evidence for a functional role in vivo.

The present data that autoantibodies similarly bound glycosylated and nonglycosylated human GM-CSF excludes the carbohydrate moiety as a component of any autoantibody epitopes. The observation that carboxymethylation completely abolished autoantibody binding suggests that autoantibodies may recognize epitopes that are composed of noncontiguous regions of the primary structure—that is, a secondary, tertiary, or quaternary structure of GM-CSF. It is possible that autoantibody binding may alter GM-CSF conformation, thus altering recognition by the monoclonal antibodies used for epitope mapping. Thus, our studies do not precisely define the target epitopes of the autoantibodies. Crystallographic analysis will likely be useful to determine the nature of the specific molecular interactions of GM-CSF and autoantibodies.

The observation that autoantibodies in most iPAP patients consistently targeted an epitope in the region of residues 78 to 94 of the mature GM-CSF molecule is of particular interest for 2 reasons. First, this region of GM-CSF is known to be functionally important.[27,28,36,37] Second, identifying an epitope that is consistently targeted by autoantibodies in iPAP patients suggests that disease severity may relate to epitope targeting by autoantibodies in a given iPAP patient rather than simply autoantibody levels. Alternatively, residues 78 to 94 may simply represent a hot spot, the targeting of which is necessary for neutralizing GM-CSF and thus for physiological function of the autoantibodies. Such functional domains of GM-CSF have been defined.[27,28,36,37] Further clinicopathologic correlations in longitudinal studies will be required to answer these questions.

Implications of impaired pulmonary GM-CSF bioactivity for AM function

The presence of abundant, high-affinity autoantibodies capable of neutralizing pulmonary GM-CSF bioactivity has important implications for the pathogenesis of iPAP. The present study demonstrates that these autoantibodies effectively eliminate GM-CSF bioactivity from the lung. The true role of GM-CSF on human AMs has not been fully elucidated. However, in mice, pulmonary GM-CSF is required to stimulate surfactant catabolism by AMs and a number of other functions strongly supporting the concept that GM-CSF is the principal factor regulating AM terminal differentiation.[12,15,16] In mice, the absence of GM-CSF or of its receptor causes PAP.[4-7] A number of similarities in the molecular, cellular, and pathophysiologic features of murine PAP in $GM^{-/-}$ mice and human iPAP suggest that the pathogenesis of iPAP also involves the disruption of pulmonary GM-CSF signaling.[1,3-7,14,16,18-21] The similarities in murine and human PAP have been, and continue to be, important for several reasons. First, the murine findings continue to identify markers of AM function that are potentially useful as surrogate markers of disease activity to test therapeutic interventions such as the administration of GM-CSF.[8,12,15] Second, and equally important, they continue to provide molecular clues regarding the potentially critical role of GM-CSF in regulating human AM functions, surfactant homeostasis, and the pathogenesis of iPAP. Our observation that autoantibodies from iPAP patients strongly inhibited the growth and development of AMs is consistent with the concept that GM-CSF may be required for terminal differentiation of human AMs

Implications of anti—GM-CSF autoantibodies for the diagnosis, management, and pathogenesis of iPAP

Our results demonstrate, in a large cohort, that autoantibodies directed at GM-CSF occur at high levels in the sera and lungs of patients with iPAP but not in those with other lung diseases or in healthy controls. This is consistent with our earlier findings[22,23] and with a subsequent report from another group.[43] These results also demonstrate in this cohort that high autoantibody levels are sensitive and specific for the diagnosis of iPAP. Thus, detecting autoantibodies by ELISA has good predictive value for iPAP and suggests the potential clinical usefulness of this assay for the diagnosis of iPAP. These results also agree with results of a latex agglutination assay recently developed by our laboratory as a screening tool for iPAP.[23] Either or both of these assays could be useful in the management of patients with iPAP to follow changes in autoantibody levels in response to therapy. However, in one report, the autoantibody titer crudely expressed in terms of total autoantibody protein concentration did not correlate well with other measures of disease severity.[32] Thus, additional studies are needed to assess the potential usefulness of autoantibody levels in the management of iPAP therapy.

Notwithstanding the potential diagnostic implications of the autoantibodies, their etiology remains unclear. Similarly, the initial or principal site of their production is unknown. The higher prevalence of iPAP in smokers suggests that cigarette smoke may be an important factor.[2] However, no mechanism has been suggested; again, further studies are needed. Future investigations should also evaluate the relationship of autoantibody titer, neutralizing capacity, and epitope mapping to the severity, duration, and remittance of the disease. Although many questions remain, the results of this study strongly support the concept that iPAP is an autoimmune disorder mediated by antibodies directed at GM-CSF.

Acknowledgments

We thank to Dr Ian Clark-Lewis (Biomedical Research Center and Department of Biochemistry and Molecular Biology, University of British Columbia), Dr Kenneth Kaushansky (Division of Hematology, University of Washington), and Dr Roberto P. Revoltella (Institute of Mutagenesis and Differentiation, C.N.R.) for their helpful technical suggestions.

References

1. Rosen SG, Castleman B, Liebow AA. Pulmonary alveolar proteinosis. N Engl J Med. 1958;258: 1123-1142.
2. Seymour JF, Presneill JJ. Pulmonary alveolar proteinosis: progress in the first 44 years. AM J Respir Crit Care Med. 2002;166:215-235.
3. Trapnell BC, Whitsett JA, Nakata K. Pulmonary alveolar proteinosis. N Engl J Med. In press.
4. Dranoff G, Crawford AD, Sadelain M, et al. Involvement of granulocyte-macrophage colony-stimulating factor in pulmonary homeostasis. Science. 1994;264:713-716.
5. Stanley E, Lieschke GJ, Grail D, et al. Granulocyte/macrophage colony-stimulating factor-deficient mice show no major perturbation of hematopoiesis but develop a characteristic pulmonary pathology. Proc Natl Acad Sci U S A. 1994;91: 5592-5596.
6. Robb L, Drinkwater CC, Metcalf D, et al. Hematopoietic and lung abnormalities in mice with a null mutation of the common beta subunit of the receptors for granulocyte-macrophage colony-stimulating factor and interleukins 3 and 5. Proc Natl Acad Sci U S A. 1995;92:9565-9569.
7. Nishinakamura R, Nakayama N, Hirabayashi Y, et al. Mice deficient for the IL-3/GM-CSF/IL-5 βc receptor exhibit lung pathology and impaired immune response, while β_{IL3} receptor-deficient mice are normal. Immunity. 1995;2:211-222.
8. Yoshida M, Ikegami M, Reed JA, Chroneos ZC, Whitsett JA. GM-CSF regulates surfactant protein-A and lipid catabolism by alveolar macrophages. AM J Physiol Lung Cell Mol Physiol. 2001;280:L379-L386.
9. Reed JA, Ikegami M, Cianciolo ER, et al. Aerosolized GM-CSF ameliorates pulmonary alveolar proteinosis in GM-CSF-deficient mice. AM J Physiol. 1999;276:L556-L563.
10. Zsengeller ZK, Reed JA, Bachurski CJ, et al. Adenovirus-mediated granulocyte-macrophage colony-stimulating factor improves lung pathology of pulmonary alveolar proteinosis in granulocyte-macrophage colony-stimulating factor-deficient mice. Hum Gene Ther. 1998;9:2101-2109.
11. Huffman JA, Hull WM, Dranoff G, Mulligan RC, Whitsett JA. Pulmonary epithelial cell expression of GM-CSF corrects the alveolar proteinosis in GM-CSF–deficient mice. J Clin Invest. 1996;97: 589-590.
12. Shibata Y, Berclaz P-Y, Chroneos Z, Yoshida H, Whitsett JA, Trapnell BC. GM-CSF regulates alveolar macrophage differentiation and innate immunity in the lung through PU.1. Immunity. 2001; 15:557-567.
13. Nishinakamura R, Wiler R, Dirksen U, et al. The pulmonary alveolar proteinosis in granulocyte macrophage colony-stimulating factor/interleukins 3/5 βc receptor-deficient mice is reversed by bone marrow transplantation. J Exp Med. 1996; 183:2657-2662.
14. Paine R III, Morris SB, Jin H, et al. Impaired functional activity of alveolar macrophages from GM-CSF–deficient mice. AM J Physiol Lung Cell Mol Physiol. 2001;281:L1210-L1218.
15. Berclaz PY, Shibata Y, Whitsett JA, Trapnell BC. GM-CSF, via PU.1, regulates alveolar macrophage FcγR-mediated phagocytosis and the IL-18/IFNγ-mediated molecular connection between innate and adaptive immunity in the lung. Blood. 2002;100:4193-4200.
16. Berclaz PY, Zsengeller Z, Shibata Y, et al. Endocytic internalization of adenovirus, nonspecific phagocytosis, and cytoskeletal organization are coordinately regulated in alveolar macrophages by GM-CSF and PU.1. J Immunol. 2002;169: 6332-6342.
17. Trapnell BC, Whitsett JA. GM-CSF regulates pulmonary surfactant homeostasis and alveolar macrophage-mediated innate host defense. Annu Rev Physiol. 2002;64:775-802.
18. Golde DW, Territo M, Finley TN, Cline MJ. Defective lung macrophages in pulmonary alveolar proteinosis. Ann Intern Med. 1976;85:304-309.
19. Harris JO. Pulmonary alveolar proteinosis: abnormal in vitro function of alveolar macrophages. Chest. 1979;76:156-159.
20. Iyonaga K, Suga M, Yamamoto T, et al. Elevated bronchoalveolar concentrations of MCP-1 in patients with pulmonary alveolar proteinosis. Eur Respir J. 1999;14:383-389.
21. Gonzalez-Rothi RJ, Harris JO. Pulmonary alveolar proteinosis: further evaluation of abnormal alveolar macrophages. Chest. 1986;90:656-661.
22. Kitamura T, Tanaka N, Watanabe J, et al. Idiopathic pulmonary alveolar proteinosis as an autoimmune disease with neutralizing antibody against granulocyte-macrophage colony stimulating factor. J Exp Med. 1999;190:875-880.
23. Kitamura T, Uchida K, Tanaka N, et al. Serological diagnosis of idiopathic pulmonary alveolar proteinosis. AM J Respir Crit Care Med. 2000;162: 658-662.
24. Tanaka N, Watanabe J, Kitamura T, Yamada Y, Kanegasaki S, Nakata K. Lungs of patients with idiopathic pulmonary alveolar proteinosis express a factor which neutralizes granulocyte-macrophage colony stimulating factor. FEBS Lett. 1999; 442:246-250.
25. Carraway MS, Ghio AJ, Carter JD, Piantadosi CA. Detection of granulocyte-macrophage colony-stimulating factor in patients with pulmonary alveolar proteinosis. AM J Respir Crit Care Med. 2000;161:1294-1299.
26. Allen G. Sequencing of proteins and peptides. 2nd ed. Amsterdam, Netherlands: Elsevier; 1989: 56-59.
27. Nice E, Dempsey P, Layton J, et al. Human granulocyte-macrophage colony-stimulating factor (hGM-CSF): identification of a binding site for a neutralizing antibody. Growth Factors. 1990;3: 159-169.
28. Kanakura Y, Cannistra SA, Brown CB, et al. Identification of functionally distinct domains of human granulocyte-macrophage colony-stimulating factor using monoclonal antibodies. Blood. 1991;77: 1033-1043.
29. Kitamura T, Tange T, Terasawa T, et al. Establishment and characterization of a unique human cell line that proliferates dependently on GM-CSF, IL-3, or erythropoietin. J Cell Physiol. 1989;140: 323-334.
30. Mosmann T. Rapid colorimetric assay for cellular growth and survival: application to proliferation and cytotoxicity assays. J Immunol Methods. 1983;65:55-63.
31. Hoshino Y, Nakata K, Hoshino S, et al. Maximal HIV-1 replication in alveolar macrophages during tuberculosis requires both lymphocyte contact and cytokines. J Exp Med. 2002;195:495-505.
32. Seymour JF, Doyle IR, Nakata K, et al. Relationship of anti–GM-CSF antibody concentration, surfactant protein A and B levels, and serum LDH to pulmonary parameters and response to GM-CSF therapy in patients with idiopathic alveolar proteinosis. Thorax. 2003;58:252-257.
33. Schoch OD, Schanz U, Koller M, et al. BAL findings in a patient with pulmonary alveolar proteinosis successfully treated with GM-CSF. Thorax. 2002;57:277-280.
34. Mclean IW, Nakane PK. Periodate-lysine-paraformaldehyde fixative: a new fixative for immunoelectron microscopy. J Histochem Cytochem. 1974;22:1077-1083.
35. Svenson M, Hansen MB, Bendtzen K. Binding of cytokines to pharmaceutically prepared human immunoglobulin. J Clin Invest. 1993;92:2533-2539.
36. Kaushansky K, Shoemaker SG, Alfaro S, Brown C. Hematopoietic activity of granulocyte/macrophage colony-stimulating factor is dependent upon two distinct regions of the molecule: functional analysis based upon the activities of interspecies hybrid growth factors. Proc Natl Acad Sci U S A. 1989;86:1213-1217.
37. Parry DAD, Minasian E, Leach SJ. Conformational homologies among cytokines: interleukins and colony stimulating factors. Mol Recognition. 1988;1:107-110.
38. Svenson M, Hansen MB, Ross C, et al. Antibody to granulocyte-macrophage colony-stimulating factor is a dominant anti-cytokine activity in human IgG preparations. Blood. 1998;91:2054-2061.
39. Svenson M, Hansen MB, Bendtzen K. Distribution and characterization of autoantibodies to interleukin 1 alpha in normal human sera. Scand J Immunol. 1990;32:695-701.
40. Ross C, Svenson M, Hansen MB, Vejlsgaard GL, Bendtzen K. High avidity IFN-neutralizing antibodies in pharmaceutically prepared human IgG. J Clin Invest. 1995;95:1974-1978.
41. Bendtzen K, Hansen MB, Ross C, Svenson M. High-avidity autoantibodies to cytokines. Immunol Today. 1998;19:209-211.
42. Rajotte D, Cadieux C, Haman A, et al. Crucial role of the residue R280 at the F'-G' loop of the human granulocyte/macrophage colony-stimulating factor receptor α chain for ligand recognition. J Exp Med. 1997;185:1939-1950.
43. Bonfield TL, Russell D, Burgess S, Malur A, Kavuru MS, Thomassen MJ. Autoantibodies against granulocyte macrophage colony-stimulating factor are diagnostic for pulmonary alveolar proteinosis. AM J Respir Cell Mol Biol. 2002;27:481-486.

ELSEVIER
SAUNDERS

Clin Chest Med 25 (2004) 593–613

CLINICS
IN CHEST
MEDICINE

Pulmonary alveolar proteinosis

Jeffrey J. Presneill, MB BS, PhD, FRACP[a], Koh Nakata, MD, PhD[b], Yoshikazu Inoue, MD, PhD[c], John F. Seymour, MB BS, FRACP[d,*]

[a]*Intensive Care Unit, Royal Melbourne Hospital, Grattan Street, Parkville 3050, Victoria, Australia*
[b]*Department of Respiratory Diseases, Research Institute, International Medical Center of Japan, 1-21-1, Toyama, Shinjuku-ku, Tokyo 162-8655, Japan*
[c]*Department of Diffuse Lung Diseases and Respiratory Failure, Clinical Research Center, National Hospital Organization Kinki-Chuo Chest Medical Center, 1180 Nagasone-cho, Sakai, Osaka 591-8555, Japan*
[d]*Division of Haematology and Medical Oncology, Peter MacCallum Cancer Centre, St. Andrew's Place, East Melbourne, VIC 3002, Australia*

Pulmonary alveolar proteinosis (PAP) (also called alveolar proteinosis, alveolar phospholipidosis, pulmonary alveolar lipoproteinosis, pulmonary alveolar phospholipoproteinosis) has been recognized for almost half a century, although descriptions of probable PAP cases can be found in the earlier medical literature. It is a rarely encountered disease reported to occur in a worldwide distribution [1], with an estimated incidence of 0.36 cases per million population and a prevalence of 3.7 per million of population [2].

At least three separate pathophysiologic mechanisms may lead to the characteristic feature of PAP: the excessive accumulation of surfactant lipoprotein in pulmonary alveoli, with associated disturbance of pulmonary gas exchange [1]. Congenital cases present in the neonatal period with life-threatening hypoxia (approximately 2% of total cases) and result from one of several genetic defects in the surfactant protein (SP)-B gene or the β_c molecule of the granulocyte-macrophage colony-stimulating factor (GM-CSF) receptor [3,4]. Secondary PAP cases (accounting for approximately 5%–10% of total cases) are associated with various underlying diagnoses, especially hematopoietic and other malignancies [5]. The most common form of PAP (more than 90% of cases) is acquired by previously healthy adults. The prognosis for adult patients with PAP varies, but disease-specific survival rate exceeds 80% at 5 years. Clinical remission also may occur either spontaneously or after therapy, although such cases may represent a quiescent disease phase rather than complete spontaneous resolution. The survival rates for adult PAP patients seem to have increased progressively in the four decades since the initial clinical description of this condition [1]. Although an effective treatment using pulmonary lavage was described soon after the recognition of PAP as a distinct entity in 1958 [6], further insights into its pathogenesis were slow to be unraveled. Fortunately, the last decade has brought new advances in laboratory and clinical research that are lifting a veil not only on the rare condition PAP but also on general aspects of pulmonary surfactant biology and innate immune defense [7].

Clinical features

Medical history

Based on several analyses of published case reports and case series that together included more than 400 patients, the common clinical features of patients with PAP are relatively well established [1,8–11]. Although the diagnosis has been reported at all ages,

This work was supported by a grant-in-aid for translational research, Japanese Ministry of Labor (H114-trans-014).

* Corresponding author.
E-mail address: John.Seymour@petermac.org (J.F. Seymour).

0272-5231/04/$ – see front matter
doi:10.1016/j.ccm.2004.04.002

a patient who has PAP is typically a previously healthy adult of median age 39 years who describes a history of slowly progressive dyspnea, with these symptoms being present for a median of 7 months. There is a wide range of possible clinical presentations, however, with 25% of patients having symptoms of 2 years or more; in up to one third of cases reported by Japanese investigators the patients were minimally symptomatic [8]. Less common symptoms include fatigue, weight loss, and low-grade fever. Cough is mostly nonproductive and may be absent in at least one fourth of patients, unless there is complicating pulmonary infection. Less than 20% of patients report hemoptysis or chest pain. Secondary pulmonary infections may occur in 13% of cases, with *Nocardia* spp. being reported most commonly [1].

There is a strong association between PAP and tobacco smoking. Overall, approximately three-fourths of patients are smokers at the onset of their disease. There is a more than a 2:1 preponderance of men among smokers, but this excess may be confounded by the often greater proportion of men who smoke in many societies, because there is no male bias among nonsmoking patients. African-American patients comprise 17% of the reported cases from North America.

Clinical examination

Physical examination is commonly remarkable for the absence of abnormal signs in the chest or elsewhere at rest. Crackles may be audible in 50% of cases, and clubbing and cyanosis have been described in approximately one fourth of some earlier case series but do not seem to be as common in recent decades [8,9,11–13].

Radiology

Chest radiography is the most useful radiologic screening test [14,15]. It reveals a pattern of bilateral diffuse alveolar densities in most patients, although interstitial, mixed, diffusely nodular, and focally dense patterns have been reported [9].

CT of the chest increases diagnostic accuracy [16] by confirming bilateral alveolar consolidation, which often appears in a "crazy-paving" pattern that consists of scattered or diffuse ground-glass attenuation with superimposed interlobular septal thickening and intralobular lines [17]. These radiologic appearances suggest PAP but are nonspecific, being found in a range of other diseases [18,19].

Pulmonary function tests

Hypoxemia caused by an increased alveolar-arterial oxygen gradient is nearly universal in symptomatic patients, and blood gas analysis together with measurement of the pulmonary diffusing capacity for carbon monoxide (D_LCO) are the most informative pulmonary function assessment tools. Among 410 published cases, the mean (± SD) P_aO_2 at diagnosis was 58.6 (15.8) mm Hg [1]. Consistent with this hypoxemia, measurements of D_LCO in a subset of patients were reported to be substantially reduced at 47% (12.7%) of the predicted normal values [9]. Lung function testing, including forced expiratory volume in 1 second (FEV_1), vital capacity (VC), and total lung capacity (TLC) may show evidence of a mild to moderate restrictive abnormality (TLC 74% ± 19.3%) [1,8,9]. These abnormalities are at least partially reversible with effective therapy, such as whole lung lavage, or during natural disease remissions [8].

Laboratory markers

Among several described abnormalities that involve raised serum levels of carcinoembryonic antigen, cytokeratin 19, and mucin KL-6 [1,11,20], the most common finding (82%) is a slight to moderate elevation of the serum level of lactate dehydrogenase (LDH). In addition to pulmonary function testing and gas exchange analysis, serial measurements of LDH in individual patients may provide an approximate index of disease activity because the LDH level and alveolar-arterial oxygen gradient show a moderate positive correlation. LDH levels may be found slightly elevated even in patients who are enjoying a clinical remission with arterial blood gas levels in the normal range. Also common in PAP are elevated serum levels of SP-A, -B and -D [1,21], the levels of which may correlate with disease severity. These findings are not specific, however, because elevated plasma levels of SPs occur in a wide range of other lung diseases [22–26]. Recently, monocyte chemoattractant protein (MCP-1) was reported to be increased in bronchoalveolar lavage fluid (BALF) from four patients [27].

Differential diagnosis

The differential diagnosis of an adult who has PAP is wide, because the clinical presentation of this syndrome is nonspecific [11,28]. Although the adult age group excludes congenital PAP as a possibility,

acquired PAP occasionally can be secondary to underlying hematopoietic malignancy [5,29], intrinsic or iatrogenic immunodeficiency disorders [30,31], lysinuric protein intolerance [32], acute silicosis, and other industrial inhalational syndromes [33].

On first presentation, acquired PAP may simulate an extensive number of conditions, including bacterial and viral pneumonia, *Pneumocystis carinii* pneumonia, acute respiratory distress syndrome, cardiogenic pulmonary edema, sarcoidosis, acute interstitial and organizing pneumonias of various etiologies, bronchiolitis obliterans organizing pneumonia, diffuse interstitial lung diseases, drug-induced pneumonitis, exogenous lipoid pneumonia, hypersensitivity pneumonitis, pulmonary hemorrhage syndromes, and bronchioalveolar carcinoma [16,18,19].

Algorithm for investigation

The diagnostic evaluation of a patient with possible PAP begins with a clinical and occupational history and physical examination that focuses on exercise tolerance and exclusion of cardiac disease or systemic disorders, such as sepsis, vasculitis, and malignancy. Blood and differential leukocyte counts help to detect any underlying hematopoietic malignancy, and blood chemistry tests, including renal and liver function assessment, help detect other systemic disorders. Moderately elevated LDH levels suggest PAP in a compatible clinical context. Plain radiography of the chest typically reveals bilateral diffuse alveolar densities; CT scans of the thorax somewhat improve the diagnostic accuracy for PAP but remain nonspecific. Lung function tests, including blood gases, lung volume measurement, and carbon monoxide gas transfer, are likely to reveal impaired gas transfer, hypoxemia, and a restrictive ventilatory defect.

Although future immunodiagnostic methods may be used to confirm a diagnosis of PAP rapidly and noninvasively (see later discussion of anti–GM-CSF antibody data), a definitive diagnosis still requires the demonstration of typical findings on either cytologic analysis of BALF or histologic examination of open or transbronchial lung biopsy specimens [34,35]. Previously, a lung biopsy was required to demonstrate alveolar filling, with excess surfactant material appearing as eosinophilic and periodic acid-Schiff positive lipoproteinaceous material with otherwise relatively preserved lung architecture and minor or absent evidence of inflammation. More recently, this approach has been supplanted in most cases by reliance on the macroscopic and microscopic appearance of returned fluid from a diagnostic fiberoptic bronchoalveolar lavage procedure [11,13,20,34,35]. PAP is associated with abundant milky bronchoalveolar lavage effluent, which on cytologic examination contains granular acellular eosinophilic proteinaceous material and foamy macrophages engorged with diastase-resistant periodic acid-Schiff positive intracellular inclusions, which also show characteristic features after Papanicolaou staining [36]. Electron microscopic demonstration of characteristic concentrically laminated phospholipid lamellar bodies can be confirmatory in cases of diagnostic doubt [1,20]. PAP rarely may be associated with considerable interstitial pulmonary fibrosis [37].

Therapeutic lung lavage

Physical removal of excess alveolar surfactant material by repeated segmental flooding with saline was first shown to be beneficial in 1960. Modern whole lung lavage using general anesthesia and single lung ventilation via a double lumen endotracheal tube has been standard therapy for several decades in symptomatic patients. This procedure usually is fairly well tolerated, with significant clinical, physiologic, and radiologic improvements expected in up to 84% of cases after the first lavage [1]. The median duration of freedom from recurrent symptoms after a single lavage treatment is 15 months, with repeat treatments commonly required [1]. Technical and patient safety aspects of whole lung lavage are well described elsewhere [11], with a total of 20 L to 40 L of saline required for the initially milky or turbid returning alveolar lavage fluid to become macroscopically clear. The rate of clearance of residual lavage fluid from the alveolar space is rapid [38], and some patients are suitable for bilateral sequential lung lavage during the same anesthetic session [11]. Recently, alternative techniques of lung lavage have been reported that use variations in fluid volume or other lavage protocols and fluid delivery directed by fiberoptic bronchoscopy [38–40].

A recommendation for whole-lung lavage therapy should be based on a skilled assessment of the relative risks and benefits of the procedure in each individual. Ultimately, however, most patients do require such treatment, with 63% of patients undergoing lavage within 5 years of diagnosis [1]. Lung lavage is associated with a 5-year survival rate from the time of PAP diagnosis somewhat superior to that of patients not afforded such treatment (± SD; 94% ± 2% versus 85% ± 5%) [1].

Outcome

Deaths directly related to PAP usually have involved respiratory failure (72%) or uncontrolled infection (18%), and most of these events occur within 1 year of diagnosis. Survival prospects for patients who have PAP seem to have improved consistently in the four decades since the condition was first described, such that survival rates approach 100% for cases reported within the last decade [1]. Spontaneous resolution has been reported in a small number of patients, and it seems likely that the disease process of PAP eventually enters a quiescent state in many other surviving patients. These observations are based on reported cases with relatively limited follow-up, however, and the true long-term outlook for these patients must be defined better.

Discovery of the role of granulocyte-macrophage colony-stimulating factor

GM-CSF was chemically purified in the late 1970s [41], and in 1984 it was one of the first human cytokines to be cloned [42]. It was an intense focus of clinical and laboratory investigation through the 1980s and 1990s because of its potent capacity to stimulate the proliferation and differentiation of neutrophilic and monocyte/macrophage lineage hematopoietic cells in vitro, an action that had remained unexplained since its recognition in 1964 [43]. This capacity provides the basis for its clinical use [44–46]. GM-CSF shares some, but not all, of its actions with granulocyte colony-stimulating factor, the other major neutrophilic hematopoietic regulator currently in clinical use [44,45]. In normal individuals, the pharmacologic administration of recombinant GM-CSF consistently leads to a dose-dependent stimulation of myeloid hematopoiesis, which results in peripheral blood neutrophilia, monocytosis, and eosinophilia [44].

Each of the previously mentioned actions requires engagement of GM-CSF with its high-affinity receptor complex. This receptor complex is a member of the cytokine class I receptor family and comprises a GM-CSF–specific α-chain and a common-β chain (β_c). The α-chain is the major binding site for the ligand and provides specificity [47,48]. The complex of the α-chain and β_c provides high affinity binding [49], and the β_c acts as the dominant signal transducer. In humans and mice, the β_c is also a component of the receptor complexes for interleukin-3 (IL-3) and IL-5 [50].

The intracellular signaling cascade induced by GM-CSF binding is complex, incompletely characterized, and shares several common components (particularly the Jak/stat pathway) with many other cytokines [51,52]. A specific conserved motif of the intracellular membrane proximal region of β_c, "box 1," is essential for Jak2 activation [53,54] and subsequent phosphorylation of stats 5a and b [55]. Although not essential for Jak2 activation, the α-chain also participates [56]. A second conserved domain of β_c is essential for the binding and activation of the adapter protein Shc, which results in the downstream activation of the GRB2/SOS/MAP kinase pathway [57]. The specific amino acid residues of β_c required for these separate functions have been characterized [58].

The capacity of hematopoietic growth factors, including GM-CSF, to influence the growth and function of hematopoietic cells in vitro has been known for more than 30 years, and these properties have been exploited in the pharmacologic administration of recombinant factors clinically [44–46]. These observations do not establish the physiologic role of these factors in vivo, however, because many factors, including cytokine concentration, temporal and spatial expression patterns, and the presence and control of effector cell populations, vary from either the experimental or pharmacologic setting. Other means of defining this physiologic role in the intact animal were required.

Gene-targeted mice that lack granulocyte-macrophage colony-stimulating factor

In 1994, two independent publications described the creation and analysis of animals that lack GM-CSF (GM-CSF$^{-/-}$) [59,60]. The phenotype was identical, with normal viability and apparently normal fertility [61] and normal steady-state hematopoiesis. The dominant abnormality, not found in GM-CSF$^{+/-}$ animals, was "alveolar-proteinosis"–like lung pathology with surfactant accumulation, which manifested as early as 4 to 8 weeks of age and was associated with an increased frequency of pulmonary infections [59,60]. Increased numbers of large, morphologically abnormal alveolar macrophages [62,63] also contained accumulated SPs and lipids. These findings suggested a critical role for GM-CSF in normal surfactant homeostasis, which was confirmed by an identical pulmonary phenotype in gene-targeted animals that lacked the signal transducing β_c chain of the GM-CSF receptor ($\beta_c^{-/-}$) [61,64,65].

Quantification of surfactant protein and lipid abnormalities

The healthy alveolar surface is lined by a thin liquid layer of surfactant, which lowers its surface tension and serves to stabilize alveoli against collapse [66]. Pulmonary surfactant is structurally heterogeneous complex lipid-protein mixture rich in phospholipids [67–69]. It is composed of 90% to 95% lipid by mass, predominantly di-saturated forms of phosphatidylcholine (SatPC) (approximately 45%), such as dipalmitoylphosphatidylcholine (DPPC), unsaturated PC (approximately 20%), and phosphatidylglycerol (approximately 5%–8%), and 5% to 10% protein [70,71]. The protein fraction contains four apoproteins, which modulate surfactant's biochemical properties and structure, and SP-A, -B, -C, and -D, named according to the chronologic order of their discovery [72]. SP-A and -D, members of Ca^{2+}-dependent carbohydrate binding collectin family, are large, water-soluble, "collagen-like" molecules [73,74], whereas SP-B and -C are small, highly lipid-soluble, hydrophobic molecules [4,75].

GM-CSF$^{-/-}$ mice have a 7.5-fold increase in bronchoalveolar lavage (BAL) total protein concentration [60] and more than tenfold increased levels of SP-A, -B, -D, and SatPC [76–80]. The total lung SatPC content of GM-CSF$^{-/-}$ mice was increased sixfold over controls, but the phospholipid composition was unaltered and the extracted surfactant functioned normally in vivo [81].

Surfactant metabolism and kinetic studies

The surfactant lipids and individual proteins are maintained in dynamic equilibrium through incompletely understood regulatory mechanisms that control synthesis, recycling, and catabolism in a coordinated fashion at the whole lung level [82–87]. Type II alveolar cells, with a large intracellular storage pool of surfactant within their lamellar bodies, are the sole source of surfactant lipid production, whereas type II cells and Clara cells can produce SPs [85,88]. In steady state, the half-life of surfactant lipids is approximately 4 to 10 hours, with approximately 50% recycled by type II cells [84,89]. Catabolism by alveolar macrophages and reuptake and catabolism by alveolar type II cells are the major routes of clearance. Historically, it was believed that the dominant catabolic pathway in most experimental animals was through type II cells, but recent studies using "residualizing" radiotracers in mice demonstrated that approximately 50% of surfactant lipids and SP-A are catabolized by alveolar macrophages [90]. Within alveolar macrophages, SP-A and DPPC are metabolized by separate pathways [91].

Detailed studies of surfactant metabolism have been conducted in GM-CSF$^{-/-}$ mice by Ikegami et al [77,79,81,92] and Reed et al [61]. The studies demonstrated no alteration in the secretion rate of surfactant lipids but impaired catabolism of SatPC [61,81]. GM-CSF$^{-/-}$ mice had gross impairment of the clearance of surfactant lipids and proteins [61,79,81]. The critical role of the macrophage in these defects was confirmed using isolated alveolar macrophages [93]. Degradation of SP-A and lipid metabolism was grossly impaired in GM-CSF$^{-/-}$ cells (approximately 10%–20% of wild-type) [93].

Phenotypic and functional studies of lung macrophages

Lung macrophages—alveolar and interstitial—are a critical component of immunologic defense of the lung and provide a pivotal link between the innate and acquired immune systems [7,94]. They are derived from bone marrow (BM) monocyte precursors [95,96] and have some limited local proliferative capacity [96], but they are responsive in vitro to M-CSF [97], GM-CSF [97–99], and IL-3 [100]. The effects of these cytokines vary, however, with differential gene expression and maturational and functional consequences [97,101]. Major functions of the alveolar macrophages include surfactant metabolism, phagocytosis of opsonized and unopsonized particles, killing of micro-organisms, and modulation of responses to local and systemic inflammatory mediators through secretion of cytokines [102,103].

A summary of the reported phenotypic and functional abnormalities of lung macrophages from GM-CSF$^{-/-}$ and $\beta_c^{-/-}$ mice and their reversibility with either local GM-CSF exposure or expression of the transcription factor PU.1 (discussed later) is provided in Table 1.

GM-CSF$^{-/-}$ cells had reduced expression of the β_2-integrins CD11a and CD11c [63] and integrins α_v and α_L [104], but CD11b and integrin α_M expression was unaltered [63,104]. The immunophenotypic profile of GM-CSF$^{-/-}$ alveolar macrophages is that of a less well-differentiated cell type, with persisting ER-MP20 and absent BM8 expression [104], which suggest incomplete terminal differentiation.

GM-CSF$^{-/-}$ alveolar macrophages have multiple defects in cytokine and mediator secretion in response to a range of stimuli. Summed leukotriene-C, -D, and -E_4 production in response to calcium ionophore

Table 1
Abnormalities described in alveolar macrophages derived from animals that lack granulocyte-macrophage colony-stimulating factor and animals that lack β_c and the capacity of either local GM-CSF expression or forced PU.1 expression to ameliorate these abnormalities

	Corrected by [reference]	
Abnormality [reference]	Local GM-CSF	Forced PU.1 expression
GM-CSF$^{-/-}$		
↑ cell diameter [62]		Yes [62]
↓ Surfactant catabolism (SP-A, DPPC, DPPE) [62,93]	Yes [93]	Partial [62]
↑ SP-A binding [93]	Yes [93]	
↓ PU.1 expression [62]	Yes [62]	
↓ BS-1 lectin binding [63]		
↓ Adhesion [62,63]	Yes [63]	Yes [62]
↓ Integrin expression [63,104]	Yes [63]	Yes [62]
↓ Mannose receptor expression [62]	Yes [62]	Yes [62]
↓ Toll-like receptor-4, and −2 expression [62]	Yes [62]	Yes [62]
↓ Fc_γ receptor expression [105]	Yes [105]	Yes [105]
↓ Phagocytosis of		
latex microspheres [62,63,104,105]	Yes [63,105]	Yes [62,104,105]
opsonized microspheres [105]	Yes [105]	Yes [105]
transferrin-coated microspheres [104]		Yes [104]
E. coli, *S. aureus*, zymosan [62]		Yes [62]
adenovirus [104]		Yes [104]
P. carinii [78]		
Abnormal cytoskeletal organization [104]		Yes [104]
↓ Leukotriene-C, -D, and E_4 production [63]	Partial [63]	
↓ PGE_2 production [106]		
↓ TNF-α secretion to LPS [62,63]	Yes [63]	Yes [62]
↓ IL-6 secretion to LPS [62]		Yes [62]
↓ IFN-γ secretion to LPS [105]		
↑ MCP-1 secretion to LPS [62]		
↓ Bactericidal activity against *E. coli*, *Streptococcus* [62]		Partial [62]
↓ IL-18 secretion to adenovirus [105]		Yes [105]
$\beta_c^{-/-}$		
↑ F4/80, CR3, and MHC class-II expression [107]		
↓ Adhesion [107]		
↓ Phagocytosis of colloidal carbon [107]		

Abbreviations: DPPC, dipalmitoylphosphatidylcholine; DPPE, dipalmitoylphosphatidy lethanolamine; IL, interleukin; MHC, major histocompatibility complex; PGE, prostaglandin E1; SP, surfactant protein; TNF-α, tumor necrosis factor-α.

was markedly suppressed, with reduced expression of the rate-limiting synthetic enzyme, 5-lipo-oxygenase activating protein [63]. Prostaglandin E_2 production also was impaired [106]. Tumor necrosis factor-α expression in response to lipopolysaccharide (LPS) exposure in vitro also was reduced [62,63]. MCP-1 was undetectable in the BAL of wild-type mice but was abundant in the BAL of GM-CSF$^{-/-}$ mice with GM-CSF$^{-/-}$ alveolar macrophages expressing MCP-1 in response to LPS, which suggests that this may contribute to the increased number of alveolar macrophages in GM-CSF$^{-/-}$ mice. The mRNA levels for the mannose receptor and Toll-like receptor-4 and -2 for LPS [108] also were reduced. Pro-inflammatory cytokine release (tumor necrosis factor-α and IL-6) in response to LPS and peptidoglycan, which is mediated via Toll-like receptor-4, Toll-like receptor-2, CD14, and MyD88, was reduced [62,63].

Numerous defects in phagocytosis have been described, including reduced uptake of fluorescein isothiocyanate (FITC)-labeled microspheres [62,63, 104,105], whether exposed in vitro or in vivo, transferrin-labeled microspheres [104] and large diameter latex spheres [104]. Phagocytosis of adenovirus, *Escherichia coli*, *Staphylococcus aureus*, *P carinii*, and zymosan by GM-CSF$^{-/-}$ cells is impaired [62,78,104]. Although phagocytosis of group B Streptococci was normal [109], bacterial killing was

grossly impaired [62]. These defects may be attributable to abnormal subcellular cytoskeletal organization [104].

GM-CSF$^{-/-}$ cells also showed specific defects in Fcγ receptor-mediated phagocytosis of IgG coated particles (opsonophagocytosis) [105], which is controlled distinctly from phagocytosis using other means (complement or mannose receptor mediated), having a specific requirement for src-family kinase activity, specifically Syk [110]. It is known that GM-CSF can enhance FcγR expression and function on alveolar macrophages [111,112]. GM-CSF$^{-/-}$ mice have a blunted interferon-γ (IFN-γ) response to LPS in vivo [105], although isolated T cells produce normal levels of IFN-γ in vitro. Berclaz et al [105] postulated that this may be caused by an indirect defect, perhaps through regulation of an "IFN-γ-releasing factor," as proposed by Noguchi et al [113], with IL-12 and IL-18 candidates for such a factor.

FcγR-mediated phagocytosis and FcγR expression were markedly reduced in GM-CSF$^{-/-}$ cells [105]. Adenoviral infection failed to stimulate FcγR expression on GM-CSF$^{-/-}$ cells, as it did in controls, but in vitro exposure to IFN-γ restored this defect. This failure of stimulation was associated with low BAL levels of IFN-γ, IL-12, and IL-18. In vivo administration of IL-18 to GM-CSF$^{-/-}$ mice after adenoviral infection or forced PU.1 expression stimulated IFN-γ production but not to wild-type levels. Either manipulation has the ability to enhance IFN-γ production, but either alone seems to be inadequate to restore this defect fully. A proposed model for the observed defect in GM-CSF$^{-/-}$ alveolar macrophage function is through reduced IL-18 production, which leads to impaired T-cell IFN-γ production and inadequate stimulation of alveolar-macrophage FcγR expression and function. The critical role for IL-18, rather than IL-12, in pulmonary IFN-γ stimulation is supported by the normal response of IL-12$^{-/-}$ mice to experimental adenoviral infection and the adverse impact of IL-18 neutralizing antibodies [114].

Recent studies have explored the mechanism of GM-CSF actions on macrophage maturation and likely molecular mediators [62]. PU.1 is an *ets* family transcription factor that regulates myeloid and B-cell development [115] and is required for the expression of GM-CSF receptor and granulocyte colony-stimulating factor receptor and myeloid maturation [116]. Adherent GM-CSF$^{-/-}$ alveolar macrophages expressed low levels of PU.1, despite the presence of high in vivo levels of M-CSF. Normal PU.1 expression specifically requires GM-CSF, but low-level expression can be mediated via a GM-CSF-independent pathway. GM-CSF exposure stimulated PU.1 expression. The abnormal morphologic appearance of GM-CSF$^{-/-}$ alveolar macrophages could be corrected by retroviral expression of PU.1, which also restored all assessed functional defects, except for the only partial restoration of surfactant metabolism and bactericidal activity. These data demonstrate that GM-CSF regulates terminal differential of alveolar macrophages through PU.1. Although PU.1 was able to restore many functions, they were not completely normalized, so another transcription factor(s) still may be involved in GM-CSF–mediated signaling in these cells.

These data are consistent with the prior demonstration that GM-CSF and PU.1 lead to expression of many overlapping genes [117,118] and that M-CSF and GM-CSF resulted in similar but distinct gene expression patterns [117]. There is a graded effect of PU.1 levels on lineage commitment, with low levels leading to B-lineage differentiation and high levels leading to macrophage lineage differentiation [119]. Spi-B, another *ets* family transcription factor not normally expressed in myeloid cells, can substitute for PU.1 in PU.1$^{-/-}$ cells, which allows full myeloid maturation to proceed [120]. A direct comparison of the phenotype and function of GM-CSF$^{-/-}$ PU.1^{+} and PU.1$^{-/-}$ Spi-B$^{+/+}$ alveolar macrophages may reveal the degree of this apparent redundancy. Other known *ets* family members do not show such redundancy in double mutant animals [121]. Other unresolved issues relating to the degree of homology between the GM-CSF$^{-/-}$ cellular phenotype and PU.1 expression include whether there are other GM-CSF–independent factors, such as IL-3 [122], that are able to induce PU.1 expression in lung macrophages, whether PU.1 expression in other lineages, such as neutrophils [123] and eosinophils [118,124], also depends on GM-CSF, and whether there are additional cellular actions of GM-CSF on lung macrophages in addition to the induction of PU.1 expression, as has been suggested from recent cell line experiments [125].

Experimental approaches to correct the pulmonary pathology in individuals who lack granulocyte-macrophage colony-stimulating factor

Bone marrow transplantation

Transplantation of wild-type bone marrow cells into irradiated $\beta_c^{-/-}$ recipients resulted in morphologic clearance of surfactant [126,127]. BAL cellularity and macrophage morphology were normalized

and BAL protein levels were corrected. Several abnormalities persisted, however, including focal alveolar macrophage aggregates, periluminal lymphocytic infiltration, and limited areas of fibrosis. Even at 6 months after transplantation, dynamic pulmonary compliance, a measure of lung distensibility, remained at approximately 50% of normal, and airway conductance, a measure of ease of airflow, was unimproved at approximately 70% of normal [127]. Pooled preparations of alveolar macrophages contained wild-type donor cells, but the actual proportions were not determined. Cellular reconstitution using recombination activating gene (RAG)-2 donors similarly improved the lung disease [126].

Pulmonary granulocyte-macrophage colony-stimulating factor expression under surfactant protein-C promoter

The SP-C gene is only expressed by pulmonary epithelial type II cells, and its promoter sequences have been used to direct transgene expression exclusively to the lung [128,129]. GM-CSF$^{-/-}$ mice with constitutive pulmonary GM-CSF overexpression were produced (GM-CSF$^{-/-}$ SP-C-GM-CSF^{+}) [76]. With pulmonary GM-CSF expression, the levels of GM-CSF were high in BAL but undetectable in serum, with no systemic effects of GM-CSF evident [62]. GM-CSF$^{-/-}$ SP-C-GM-CSF^{+} mice developed no morphologic features of surfactant accumulation. Alveolar macrophages from GM-CSF$^{-/-}$ SP-C-GM-CSF^{+} mice were proliferating by proliferating cellular nuclear antigen (PCNA) staining, consistent with the mitogenic effects of GM-CSF, and had increased numbers of proliferating type II cells [130] with "alveolar wall hyperplasia."

Adenoviral granulocyte-macrophage colony-stimulating factor gene transfer

Adenovirus is a commonly used vector for therapeutic gene delivery [131]. The duration of expression has been limited by immune clearance of virally infected cells [132], with the dominant site of expression influenced by the route of delivery, cellular expression of the coxsackie-adenovirus receptor, and the degree of host immunosuppression [131,132]. The intratracheal (IT) administration of an adenoviral construct that contained the GM-CSF gene was studied in GM-CSF$^{-/-}$ mice after immunosuppression using an anti–T-cell receptor antibody [133]. Pulmonary GM-CSF expression was confirmed by ELISA of BAL at 1 week but declined to undetectable levels by 3 weeks. GM-CSF mRNA was still detected by reverse-transcriptase polymerase chain reaction (rtPCR) up to 5 weeks, however. Histologic improvement in surfactant accumulation was evident by 5 weeks.

Aerosolized administration of granulocyte-macrophage colony-stimulating factor

A human clinical study has shown aerosolized GM-CSF to be well tolerated and bioactive, which makes this delivery route clinically appealing for pulmonary-directed therapies [134]. When GM-CSF$^{-/-}$ mice received an aerosol of GM-CSF solution 5 days a week for 4 or 5 weeks they had marked

Table 2
Comparison of pathologic features of alveolar macrophages from mice that lack granulocyte-macrophage colony-stimulating factor and patients with acquired pulmonary alveolar proteinosis

Finding in GM-CSF$^{-/-}$ mice [reference]	Corresponding data in patients with acquired PAP [reference]
↑ Cell diameter [62]	Yes [27,135,136]
↓ PU.1 expression [62]	Yes [137,138]
↓ Adherence [62,63]	Yes [136]
↓ Phagocytosis of	
-latex microspheres [62,63,104,105]	Yes [139]
-*S. aureus* [62]	Yes [140,141]
↑ MCP-1 secretion to LPS [62]	High BAL: MCP-1 levels [27]
↓ Bactericidal activity against *Candida* [62]	Yes [136,140]
↓ αNAE staining [77,133]	Yes [136]
↓ Toll-like receptor-4, and −2 expression [62]	Yes [138]
↓ Mannose receptor expression [62]	Yes [138]
↓ Fc_{γ} receptor expression [105]	Yes [138]
Normal phagocytosis of opsonized sheep red blood cells in $\beta_c^{-/-}$ mice [107,142]	Yes [143]

but incomplete improvement in surfactant accumulation. This improvement was reflected in BAL SP-B levels. Alveolar-macrophage morphology was improved.

Interpretation and overview

In aggregate, these studied provide major insights into the cell population responsible for the surfactant accumulation in GM-CSF$^{-/-}$ and $\beta_c{}^{-/-}$ mice. It is clear that local GM-CSF effects are adequate for normal surfactant homeostasis without requiring any systemic GM-CSF actions in the BM and that the effectors within the lung are nonlymphoid hematopoietic-derived cells, presumably myeloid cells and their progeny, including alveolar macrophages. The aerosol and adenoviral gene transfer data demonstrate that a significant time delay is required for this improvement to be manifest and that low levels of GM-CSF are probably adequate, which potentially explains the lack of abnormalities in GM-CSF$^{+/-}$ animals. It is unclear whether the observed delay implies a lag period necessary for macrophage maturation or the time required to degrade the large amount of accumulated surfactant. The transplant data clearly demonstrate that restoration of alveolar macrophage function is adequate for surfactant homeostasis; the other models reveal significant GM-CSF actions on type II cell number and function.

These studies clearly suggest strong functional similarities between the phenotype of GM-CSF$^{-/-}$ mice and the human condition of alveolar proteinosis. They demonstrate several abnormalities at a cellular and functional level that are present in GM-CSF$^{-/-}$ animals and suggest that analogous defects may exist in patients with alveolar proteinosis (Table 2).

GM-CSF$^{-/-}$ animals also have several relatively subtle systemic immunologic abnormalities. They manifest impaired stimulation of T cells to induce IFN-γ secretion [113,144], potentially caused by impaired IL-18 production. Generally, GM-CSF$^{-/-}$ mice have a reduced susceptibility to experimentally induced autoimmune disorders [145–148] despite an increased incidence of late spontaneous autoimmunity in some strain backgrounds [149]. There is less severe functional impairment of macrophages from sites other than the lung [149,150] and remarkably apparently normal neutrophil function [107,109,142]. The possible presence of such features has not been explored in patients with PAP.

These abnormalities manifest at the level of the whole animal as an impaired ability to resolve a range of infections under certain conditions, which usually implicates cellular effectors other than neutrophils, including *Listeria* [151], group B streptococcus [109], adenovirus [104], *P carinii* [78], and malaria [152].

Granulocyte-macrophage colony-stimulating factor antibodies and new diagnostic tests

Most reported serologic tests for PAP are based on small series of patients and lack specificity. No specific marker for the serologic diagnosis of PAP was available until the recent discovery of the autoantibody against GM-CSF. The discovery of this antibody provided the explanatory link between the pulmonary phenotype in GM-CSF$^{-/-}$ mice and patients with PAP.

History and assays for anti–granulocyte-macrophage colony-stimulating factor autoantibody

In 1999, the specific finding of neutralizing autoantibodies against GM-CSF in the BALF from 11 Japanese patients with idiopathic PAP was first reported [153]. Subsequently, examination of sera from 24 patients with "idiopathic" PAP from five different countries showed that the autoantibody was consistently and specifically present [154,155]. Detection of the autoantibody in sera can be used for the diagnosis of "idiopathic" PAP. To establish a simple and convenient methodology, several assays have been developed. The details of these assays have been published previously [154–156], and the pertinent aspects of their performance are briefly summarized. The assays are as follows:

1. Blot assay with ^{125}I-GM-CSF
2. Latex agglutination test using latex beads coupled with recombinant human GM-CSF
3. Bioassay of growth inhibition of a GM-CSF–dependent cell line by the autoantibody

Blot assay with ^{125}I-granulocyte-macrophage colony-stimulating factor

This assay is based on a technique of so-called "West-Western blotting." The serum sample to be tested for the presence of the autoantibody is loaded in an acrylamide gel followed by transfer onto a membrane, which is then incubated with radiolabeled GM-CSF. This procedure is relatively labor intensive and time consuming and requires gel-electrophoresis before protein transfer to the membrane, overnight incubation, and prolonged autoradiography (Fig. 1).

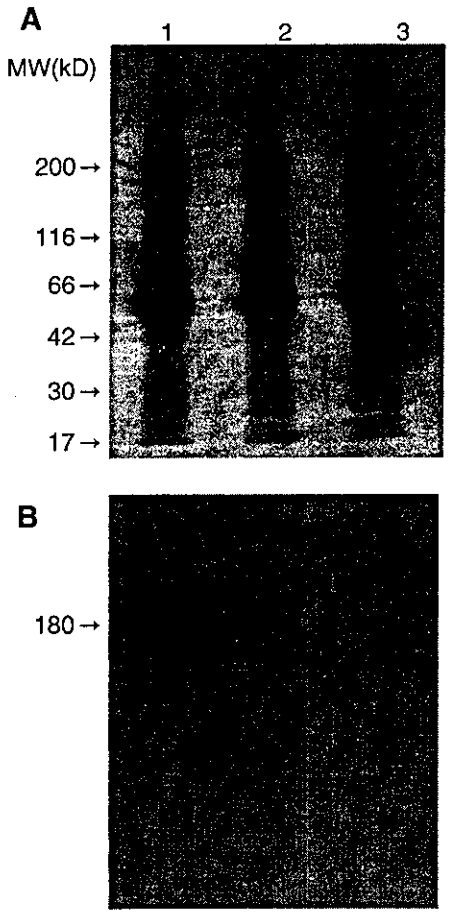

Fig. 1. Detection of the autoantibody using blot assay with 125I-GM-CSF. Serum problems are electrophoresed, transferred to membranes, stained with Coomassie brilliant blue (*A*), incubated with ^{125}I-GM-CSF, and autoradiographed (*B*). Serum proteins were incubated with ^{125}I-GM-CSF in the presence (Lane 2; 50-fold, Lane 3; 500-fold) or the absence (Lane 1) of non-radioactive GM-CSF.

The resulting autoradiograph shows the specific binding of the autoantibody, which can be reduced competitively by preincubation with excess nonradioactive GM-CSF.

Latex beads coupled with recombinant human granulocyte-macrophage colony-stimulating factor

This method is based on the passive agglutination of antibodies with their corresponding antigens, which is widely used for detection of various antibodies in serum, urine, or other biologic materials. Latex beads (1 μm diameter) are coupled with recombinant human GM-CSF. These coupled beads are transferred to a round bottom microplate and incubated for 24 hours. Agglutination is detected by visual inspection. The titer of the autoantibody can be defined using serial dilution.

Using this latex bead assay, sera from 110 persons, including 24 patients with idiopathic-PAP, 4 with secondary PAP, 2 with congenital PAP, 40 control patients with other lung diseases, and 40 normal control subjects were examined (Fig. 2). Agglutination was observed in all sera from patients with idiopathic PAP and 2 of 40 sera from normal subjects. It was negative in sera from 4 patients with secondary PAP, 2 patients with congenital PAP, and 40 patients with other lung diseases. The overall sensitivity was 100% and specificity was 98% (χ-square value = 99.177; $P<0.0001$). These data established that the latex agglutination test is a reliable method for the serologic diagnosis of idiopathic-PAP (Table 3).

Bioassay of growth inhibition of a granulocyte-macrophage colony-stimulating factor–dependent cell line

A GM-CSF, IL-3, and IL-5–dependent cell line, TF-1, provides a useful tool for determining the presence of biologically active concentrations of these cytokines. Using this cell line, the specific inhibition of GM-CSF bioactivity by the autoantibody can be estimated. This assay requires 3 days culture of TF-1 cells in medium-containing recombinant human GM-CSF either with or without diluted serum to be

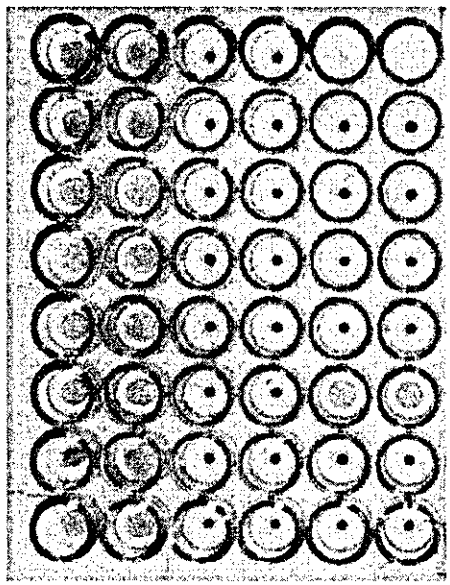

Fig. 2. Latex agglutination test for serologic diagnosis of I-PAP. Latex beads agglutinated by the autoantibodies fall to the bottom of the well in a fine mat. In contrast, beads that are not agglutinated fall to the bottom in a button. A distinct "dot" is observed as a negative result. Agglutination was observed in duplicate sera from eight patients with "idiopathic" PAP (2 left columns) but not in duplicate sera from eight patients with other lung diseases (2 middle columns) or in six of eight normal subjects (2 right columns).

Table 3
The latex agglutination for serologic diagnosis of idiopathic pulmonary alveolar proteinosis

	Latex agglutination test	
	Positive	Negative
I-PAP (n = 24)	24	0
S-PAP (n = 4)	0	4
C-PAP (n = 2)	0	2
Other lung diseases (n = 40)	0	40
Normal subjects (n = 40)	2	38

Abbreviation: S-PAP, secondary PAP.

assayed. TF-1 cell survival is then measured using the 3-[4,5-dimethylthiazol-2yl]-2,5-diphenyltetrazolium bromide assay, a chromogen that provides a visual readout of viable cell number (Fig. 3).

Determination of the serum autoantibody titer

The assays described are convenient and adequately sensitive for detection of the autoantibody, but they are semi-quantitative and imprecise in determining antibody titer. To improve this, an ELISA system using purified autoantibody as a standard was developed. Serum autoantibody against GM-CSF was assayed centrally in a blinded manner [155]. The concentration of purified autoantibody was determined by a sandwich-type ELISA with nonlabeled and peroxidase-labeled anti–human IgG antibodies, using human IgG as a standard for quantitative analysis. After appropriate dilution, incubation, and washing, any antibodies captured by recombinant GM-CSF are detected by peroxidase-labeled anti–human IgG $F(ab)_2$ antibody. The lower detection limit of the assay is 3 μg/mL.

Using this assay, the autoantibody was detected in sera from all patients with "idiopathic" PAP (n = 165) but not in any normal controls (n = 19) and other lung diseases (n = 10) consistent with the previous report (Fig. 4) [155]. This assay performs similarly well on BAL fluid, being positive in all patients with idiopathic PAP (n = 34) but negative in all normal controls (n = 18) and other lung diseases (n = 14). There was no significant difference between the serum levels of the autoantibody according to gender, age, smoking history, disease duration, or the presence of symptoms.

In contrast to the lack of correlation between serum autoantibody concentration and pulmonary findings, the serum levels of KL-6 and carcinoembryonic antigen (CEA) levels are clearly correlated with D_LCO in this cohort (Fig. 5).

Specificity and sensitivity of the autoantibody for serologic diagnosis of idiopathic pulmonary alveolar proteinosis

Fig. 6 shows the specificity and sensitivity of the titer of serum KL-6, CEA, SP-A, SP-D, MCP-1, and the autoantibody against GM-CSF for serologic diagnosis in 25, 5, 10, 9, 5, and 42 subjects with

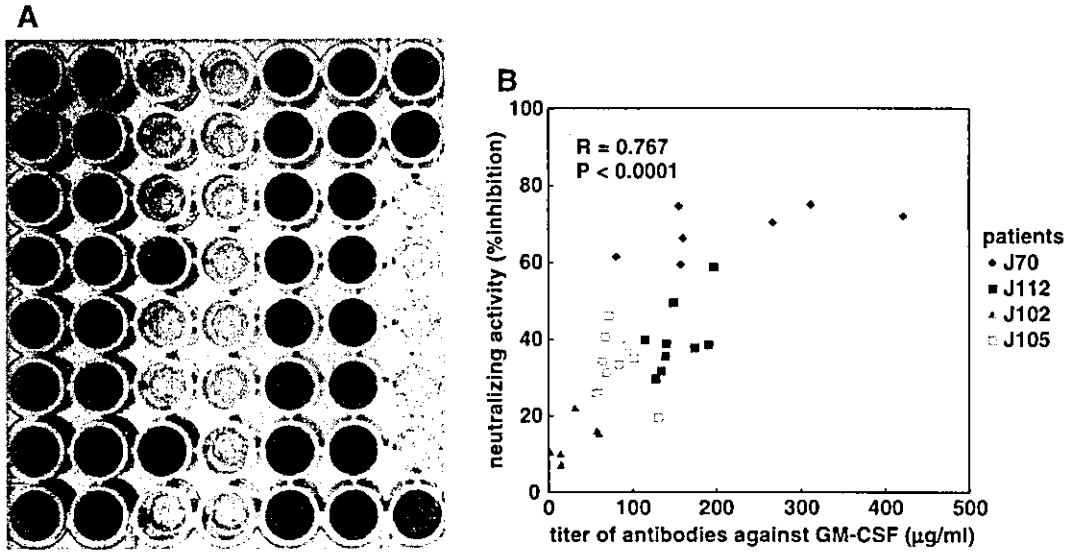

Fig. 3. (*A*) Formation of formazan by TF-1 cells after incubation with GM-CSF with or without diluted serum from a patient with idiopathic PAP. (*B*) Correlation between the neutralizing activities and titers of the autoantibodies in the serial sera formed clusters in each patient.

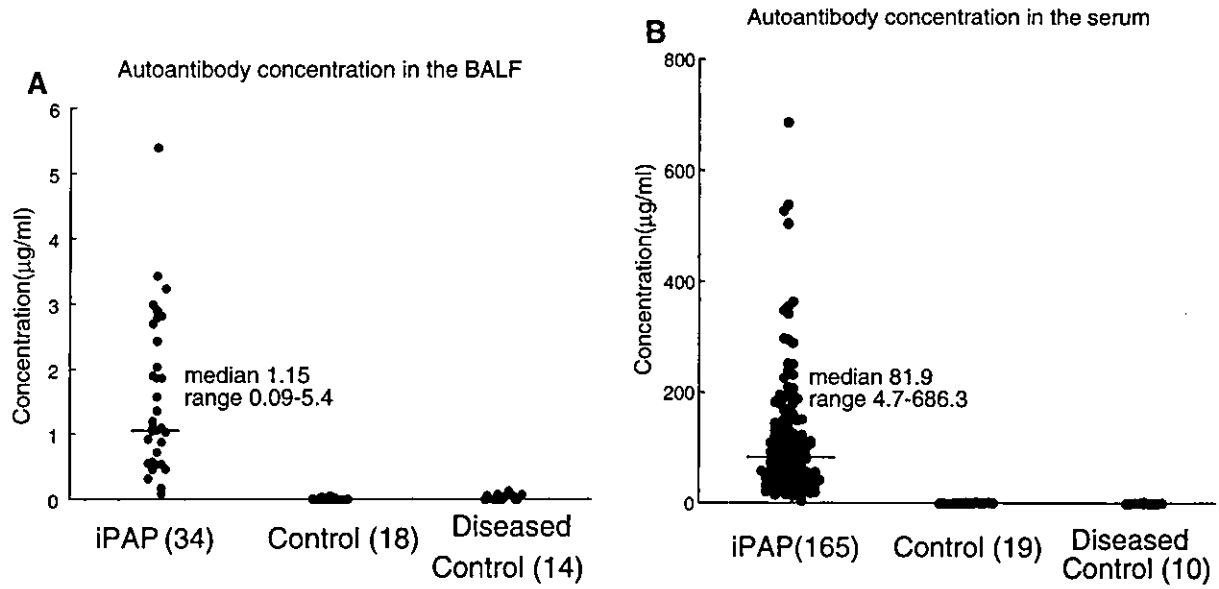

Fig. 4. (*A, B*) Titers of the autoantibody against GM-CSF in Japanese patients with idiopathic PAP.

idiopathic PAP, secondary PAP, idiopathic pulmonary fibrosis, sarcoidosis, collagen-vascular diseases, and normal controls, respectively. The receiver-operator characteristic curves indicate that regardless of level, the presence of the autoantibody achieves high specificity and sensitivity when it is applied for the serologic diagnosis of idiopathic PAP.

Role of granulocyte-macrophage colony-stimulating factor in alveolar macrophage development and function

Alveolar macrophages from GM-CSF$^{-/-}$ mice do not express the differentiation-inducing transcription factor, PU.1. Retroviral-mediated PU.1 expression in cultured GM-CSF$^{-/-}$ alveolar macrophages corrects most of the observed defects, including SP catabolism. GM-CSF plays a critical role in surfactant homeostasis by acting locally in the murine lung and stimulating alveolar macrophage terminal differentiation.

GM-CSF in the lung also is likely to be critical for surfactant homeostasis in humans, as supported by several observations. First, pathologic features of human PAP strongly resemble those of GM-CSF$^{-/-}$ mice. Second, alveolar macrophages in murine and human PAP share several similar morphologic and functional abnormalities (see Table 2). Third, BALF and serum from patients with idiopathic PAP contain high concentration of neutralizing autoantibodies against GM-CSF. Fourth, the presence of the autoantibody to GM-CSF is highly specific for idiopathic PAP. Because physiologic levels of GM-CSF protein

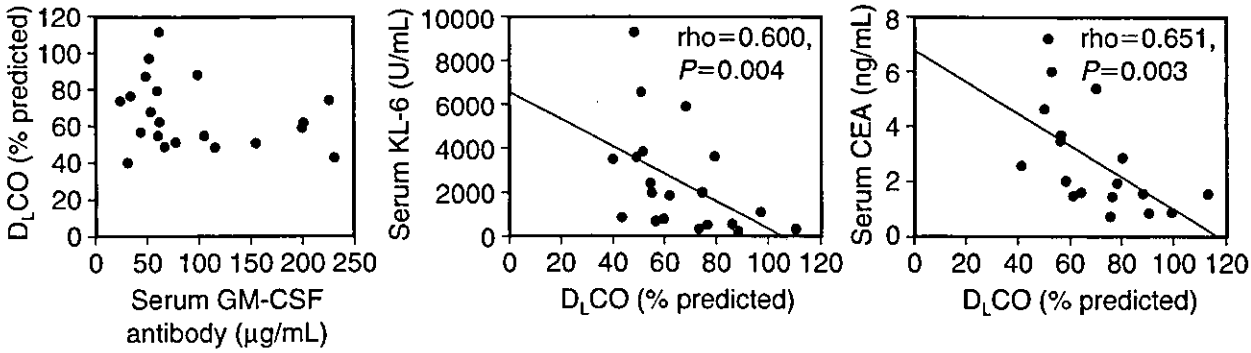

Fig. 5. Correlation between D_LCO (% predicted) and the titer of the autoantibody, serum KL-6, and between serum CEA in 25 patients with "idiopathic" PAP.